Deep–Sea Research II 227 (2026) 105621

Contents lists available at ScienceDirect

Deep-Sea Research Part II

journal homepage: www.elsevier.com/locate/dsr2

Drivers of benthic megafauna community dynamics in the Fram Strait, Arctic Ocean: Insights from the HAUSGARTEN observatory (2016-2021)

Lilian Boehringer [a,*], Melanie Bergmann [a], Christiane Hasemann [a], James Taylor [b], Jennifer Dannheim [a]

[a] Alfred Wegener Institute, Helmholtz Centre for Polar and Marine Research, 27570, Bremerhaven, Germany
[b] GEOMAR Helmholtz Centre for Ocean Research Kiel, 24105, Kiel, Germany

ARTICLE INFO

Keywords:
Long-term ecological research
Arctic ocean
Deep sea
Epibenthic megafauna
Image analysis
Polar regions
Seafloor
Benthos

ABSTRACT

Benthic megafauna communities in the Arctic Ocean play a vital role in deep-sea ecosystem functioning by influencing the local biogeochemistry and the global carbon cycle. Their community structure is largely driven by phytodetrital fluxes from the surface ocean, increasing their susceptibility to environmental change. This study assessed short-term variability in benthic megafauna community composition, taxonomically and functionally, across three stations (N3, HG-IV, S3) situated within the lower bathyal zone (~2500 m) at the LTER HAUSGARTEN site, in relation to environmental parameters such as biogenic sediment components and habitat features. The analysis was based on image data and sediment samples collected in consecutive years from 2016 to 2021. Additionally, long-term changes in the density of four selected taxa were examined by comparing two periods: 2002/2004-2015 (literature-based) and 2016-2021 (this study). Over the six-year period, the community structure showed considerable temporal variability, primarily driven by changes in the density of the opportunistic sea cucumber *Elpidia heckeri*. Environmental parameters explained spatial variation across stations more effectively than temporal variation across years. Long-term analyses revealed a general decline in density of the selected taxa, with average density decreases ranging from 28% for a crinoid to 93% for a soft coral. These findings highlight the dynamic nature of Arctic benthic megafauna communities and their complex responses to local environmental change. The pronounced temporal fluctuations and substantial population declines underscore the urgent need to extend time-series studies both temporally and spatially to enable accurate predictions of the future state of Arctic deep-sea ecosystems.

1. Introduction

1.1. Benthic megafauna in the Arctic Ocean

Epibenthic megafauna inhabit the sediment-water interface, and many of these are deposit or suspension feeders and are thus directly dependent on the downward flux of food particles through the water column. In fact, benthic communities as a whole are strongly influenced by surface ocean processes, with patterns of distribution, abundance, and biomass on the seafloor often reflecting conditions in the upper ocean (Smith et al., 2009). The diversity (Campanyà-Llovet et al., 2017; Meyer et al., 2013) and density (Bergmann et al., 2011; Taylor et al., 2016) of benthic megafauna are closely linked to both the quantity and quality of organic matter reaching the seafloor, thereby shaping benthic community structure and ecological function (Piepenburg et al., 1996; Taylor et al., 2017).

In the Arctic Ocean, benthic megafauna play a key role in deep-sea ecosystems, acting as ecosystem engineers (Jones et al., 1994) by regulating community dynamics, structuring habitats (Buhl-Mortensen et al., 2010; Quéric and Soltwedel, 2007; Soltwedel and Vopel, 2001), and influencing benthic food webs (Bergmann et al., 2009; Iken et al., 2001; Thistle, 2003; Van Oevelen et al., 2011). Through bioturbation and the processing of organic matter, they significantly impact local biogeochemical cycles (Bett et al., 2001; Soltwedel et al., 2019b; Wheatcroft et al., 1989), ultimately contributing to the global carbon cycle (Klages et al., 2004).

Due to the pronounced seasonality in light availability and primary production in the Arctic Ocean, the flux of particulate organic matter –

This article is part of a special issue entitled: LTER HAUSGARTEN published in Deep-Sea Research Part II.

* Corresponding author.
E-mail address: lilian.boehringer@awi.de (L. Boehringer).

https://doi.org/10.1016/j.dsr2.2026.105621
Received 9 January 2025; Received in revised form 1 March 2026; Accepted 3 March 2026
Available online 3 March 2026

including rapidly sinking ice-associated algae – varies considerably throughout the year, leading to natural fluctuations in food availability for benthic communities (Bluhm et al., 2011; Hoste et al., 2007; Taylor et al., 2017; von Appen et al., 2021). Additionally, nutrient limitation in the euphotic zone, caused by strong water column stratification and seasonal sea-ice cover, further modulates the export of phytodetritus to the seafloor (Bluhm et al., 2015; Gosselin et al., 1997; Gradinger, 2009; von Appen et al., 2021). Variability in both the sources and delivery pathways of phytodetrital matter influences the nutritional landscape of the benthic environment (Mintenbeck et al., 2007; Turner, 2002).

1.2. Long-term trends in benthic megafauna communities

The composition of benthic communities in the deep sea is not static but undergoes constant changes. These changes can unfold at differing time scales ranging from intra-annual to decadal dimensions, as observed at long-term observatories in the Atlantic Ocean at the Porcupine Abyssal Plain (Bett et al., 2001; Billett et al., 2010), in the Arctic Ocean at the HAUSGARTEN observatory (Bergmann et al., 2011; Meyer-Kaiser et al., 2025; Taylor et al., 2017; von Appen et al., 2021), and in the Pacific Ocean at Station M, where cyclical changes in echinoderm abundance over 30 years were observed (Kuhnz et al., 2014, 2020). Drivers of such variations can be natural cycles as well as climate-change-induced changes in environmental conditions. This is especially true for the Arctic Ocean, which will be affected by climate change in several complex ways (Henson et al., 2017), such as sea ice melting at rates faster than expected (Stammerjohn et al., 2012) and thinner and broken up ice sheets increasing sunlight penetration, triggering enhanced phytoplankton blooms in certain areas (Ardyna and Arrigo, 2020; Assmy et al., 2017). In addition, weaker upper ocean stratification will likely cause a delayed phytoplankton spring bloom (Mayot et al., 2020), which may affect zooplankton dynamics (Søreide et al., 2010) and will inevitably lead to changing environmental conditions for benthic communities. Indeed, the benthic megafauna communities in the Arctic Ocean were observed to vary dynamically, exhibiting intra-as well as inter-annual variation at differing time points between 2002 and 2015 (Bergmann et al., 2011; Meyer et al., 2013; Meyer-Kaiser et al., 2025; Taylor et al., 2017). To obtain a more complete understanding of mechanisms driving change in benthic communities and thus predicting potential future communities, it is important to extend these investigations to obtain long-term observations continuing beyond natural cycles, with natural cycles extending from interannual to multidecadal time scales and long-term trends continuing beyond as a result of anomalous environmental conditions (Henson et al., 2016).

1.3. Long-Term Ecological Research observatory HAUSGARTEN

In order to provide such long-term observations, the Alfred Wegener Institute, Helmholtz Center for Polar and Marine Research, Germany, established the Long-Term Ecological Research (LTER) observatory HAUSGARTEN in the Fram Strait, Arctic Ocean in 1999 (Soltwedel et al., 2005). It currently consists of 21 stations, sampled every year during scientific expeditions, with additional year-round time-series data collected by mooring arrays and benthic landers and crawlers (Soltwedel et al., 2005, 2016). The hydrography of the Fram Strait is characterized by the inflow of relatively warm and nutrient-rich Atlantic water into the central Arctic Ocean via the eastern part as the West Spitsbergen Current (WSC; Beszczynska-Möller et al., 2012). Cooler and less saline polar waters exit the Arctic Ocean in the western Fram Strait as the East Greenland Current (EGC; de Steur et al., 2009). The percentage of sea-ice cover in the region is strongly influenced by these circulations, with high annual sea-ice variability and seasonal shifts in the ice edge of 50-100 km (Steele and Ermold, 2015).

The HAUSGARTEN observatory provides a unique opportunity to continue the study on interannual dynamics of benthic megafauna communities in the Arctic Ocean. This study is a continuation of the time-series analyses, which started in 2002/2004 (Bergmann et al., 2011; Soltwedel et al., 2009) and continued until 2015 (Taylor et al., 2017). Here we analyzed the megafauna communities at three stations in the Fram Strait (N3, HG-IV, S3) from 2016 to 2021 to identify short- and long-term trends in polar community dynamics. We aim to address the following questions: (1) Are there short-term variations in megafaunal community parameters during the six-year study period? (2) Can overarching trends for all stations be identified and accounted for by environmental variables, such as biogenic sediment compounds (e.g., organic carbon content and phaeopigments) and habitat features (e.g., burrows, shells, and stones)? (3) Is there a clear pattern in the density change of selected megafauna taxa when comparing the two time periods, 2002/2004-2015 (literature-based) and 2016-2021 (this study)?

2. Methods

2.1. Study site

Benthic megafauna communities were studied at three stations (Fig. 1) located along a latitudinal transect at the HAUSGARTEN observatory, characterized by contrasting annual sea-ice cover. These stations are key stations in the HAUSGARTEN long-term observations, where numerous multidisciplinary annual measurements and studies are conducted (Soltwedel et al., 2005, 2016). At each station, annual photographic surveys following a pre-set transect were conducted (Fig. 1). The northern station N3 (79°35.71′N 5°12.57′E) is located near the ice edge and is therefore regularly covered by sea ice and exposed to melting events. The photographic surveys followed a south-easterly direction at a depth ranging between 2600 and 2720 m. The central station HG-IV (79°4.82′N 4°4.74′E) is occasionally covered by sea ice. The photographic surveys followed a south-westerly direction at an increasing depth from 2300 to 2600 m. The southernmost station S3 (78°37.2′N 5°1.03′E) remains ice-free throughout most of the year. The photographic surveys followed an easterly direction with a depth ranging between 2290 and 2312 m. The seafloor at all stations is characterized by soft sediments (Soltwedel et al., 2005) with regular occurrences of dropstones, large stones released by melting icebergs that form hard-bottom structures (MacDonald et al., 2010; Meyer et al., 2016; Schulz et al., 2010). Differences in benthic community composition within photographic surveys were only reported for the central station HG-IV and attributed to the large depth difference between the start and end of the surveys (Taylor et al., 2016). Therefore, only images located at the deeper end of the photographic surveys at HG-IV (~2600–2450 m) were used for this study.

2.2. Photographic survey

Photographic surveys have become a common non-invasive method to study benthic megafauna communities (Schoening et al., 2020), as surveys based on physically collected samples, such as trawls, have been found to categorically underestimate larger and less abundant megafauna (Piepenburg et al., 1995). The photographic surveys included in this study at N3, HG-IV, and S3 were conducted in consecutive years from 2016 to 2021 during the expeditions PS99 (Soltwedel, 2016), PS107 (Schewe, 2018), PS114 (von Appen, 2018), PS121 (Metfies, 2020), and PS126 (Soltwedel, 2021) aboard the German icebreaker RV Polarstern (Knust, 2017) and MSM77 (Soltwedel et al., 2019a) and MSM95 (Purser et al., 2020) aboard RV Maria S. Merian (Table 1). All surveys were conducted with towed camera systems – the Ocean Floor Observation System (OFOS) in the years 2016-2019 and the Ocean Floor Observation and Bathymetry System (OFOBS) in 2020 and 2021. The OFOBS is a more advanced version of the OFOS, equipped with an additional sidescan bathymetry sonar system but relying on the same high-resolution photo camera (iSiTEC, CANON EOS 5D Mark III) as its predecessor OFOS (see Purser et al. (2019) for a detailed description of

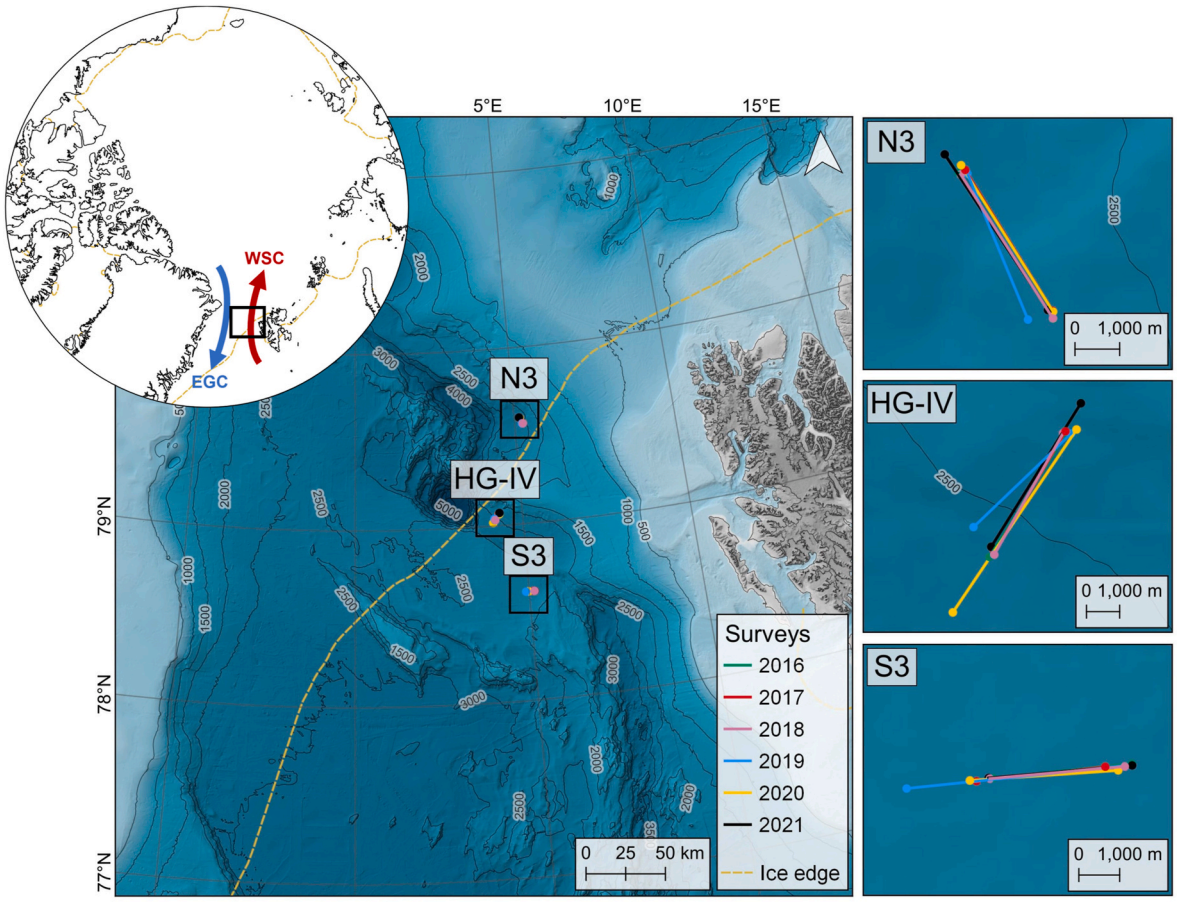

Fig. 1. Maps of the LTER HAUSGARTEN observatory in the Fram Strait west of Svalbard. The overview map on the left shows the Arctic Ocean and the location of the observatory (black rectangle) with the ice edge shown based on a 30-year average of the month of August (yellow-dashed line) and the two main current systems: East Greenland Current (EGC - blue) and West Spitzbergen Current (WSC - red). The main map shows the location of the three stations investigated here: N3, HG-IV, and S3. Annual photographic surveys were conducted at each station from 2016 to 2021 (see color code) and are depicted on the right. Map source: IBCAO v. 4.0 (Jakobsson et al., 2020). Data for the ice edge was downloaded as a sea-ice frequency isoline from 1992 to 2021 (Itkin et al., 2014).

OFOS and OFOBS), thus enabling intercomparisons between photographs taken with either camera system. At all stations, the camera system was deployed for ~5 h at a ship speed of ~0.5 knots to cover a minimum distance of four km for each deployment at a target altitude of 1.5 m above the seafloor. This altitude enables the identification of megafauna ≥1.5 cm in size and reduces the bias of varying image resolutions when strictly adhering to it (Schoening et al., 2020). The still camera was automatically triggered at 20-s intervals to avoid spatial overlap of images and replication of faunal observations.

2.3. Megafauna and habitat feature assessment

The image analysis was conducted using the annotation software biigle.de (Langenkämper et al., 2017). All image data used in this study were subjected to rigorous selection criteria, such as good illumination, good focus, the absence of sediment clouds, and an image area ranging between 3.5 and 6 m^2 to adhere to common standards for imaging studies (Durden et al., 2016b). The area of each image was calculated based on three laser points visible in each image with an equilateral distance of 50 cm. The distorted, darker corners of each image were cut before the image area calculations by defining an 'export area' for each photographic survey, which was projected onto each image and only included the well-illuminated and well-focused part in the center of each image. Images matching those criteria were selected in order of increasing export area until their cumulative area reached approx. 150 m^2 per photographic survey. This resulted in the exclusion of a large number of images and the usage of approx. 40 images per year and station (Table 1).

Discernible megafauna organisms (≥1.5 cm in size) were annotated and classified to the lowest possible taxonomic level using a taxa key derived from previous megafauna observations (Bergmann et al., 2009; Taylor et al., 2017). Some organisms could only be classified as morphotypes, but were treated as individual taxa. Unidentified organisms were annotated but excluded from the following analyses. To minimize potential bias associated with image sequence or prior knowledge, all images were randomly sorted before annotation to avoid any systematic influence of sampling order (Durden et al., 2016a). To reduce individual error and mitigate inter-observer variability, each image was annotated three times by the same annotator, with time intervals between sessions to minimize memory effects. Finally, all annotations were re-examined using the Label Review Grid Overview tool (LARGO) provided within biigle.de. This tool displays all annotations with the same label in a grid overview, thereby enabling direct comparison and review between annotations of different years and stations.

In addition, habitat features were annotated on each image. These included: Specimens of *Bathycrinus* cf. *carpenterii* with retracted feeding arms which were annotated as '*Bathycrinus* stalk'; small burrows in the sediment either created by the burrowing amphipod *Neohela lamia* or of unknown origin were annotated as 'burrow'; tests of the sea urchin *Pourtalesia jeffreysi* were annotated as 'echinoid test'; bivalve and gastropod shells showing no signs of the living organism were annotated as 'shell'; dead sponge stalks of either *Caulophacus arcticus* or *Cladorhiza gelida* were annotated as 'sponge debris'; large stones (>50 mm) were annotated as 'dropstones'; small stones (<50 mm) were annotated as

Table 1
Summary of photographic surveys conducted at stations N3, HG-IV, and S3 of the HAUSGARTEN observatory from 2016 to 2021. Lat: Latitude; Lon: Longitude; No: Number.

Year	Expedition	Camera system	Station	Deployment number	Date (dd/mm/yy)	Lat (N)	Lon (E)	Depth (m)	No. images taken
						Start	Start		(No. images analyzed)
						End	End		
2016	PS99	OFOS	N3	56-1	05/07/16	79°35.91′	5°10.00′	2718	480 (40)
						79°34.06′	5°15.39′	2591	
			HG-IV	42-10	26/06/16	79°3.86′	4°17.27′	2352	548 (39)
						79°1.99′	4°10.04′	2575	
			S3	41-11	25/06/16	78°37.00′	5°0.32′	2312	461 (41)
						78°37.03′	5°9.6′	229	
2017	PS107	OFOS	N3	36-6	10/08/17	79°34.16′	5°15.40′	2601	466 (41)
						79°35.94′	5°10.46′	2713	
			HG-IV	6-12	28/07/17	79°2.03′	4°10.41′	2564	523 (39)
						79°3.92′	4°17.30′	2352	
			S3	2-20	26/07/17	78°36.98′	4°59.19′	2313	375 (40)
						78°37.02′	5°7.83′	2293	
2018	PS114	OFOS	N3	33-3	23/07/18	79°35.89′	5°10.13′	2786	764 (38)
						79°34.07′	5°15.38′	2658	
	MSM77		HG-IV	35-4	27/09/18	79°3.76′	4°17.16′	2365	870 (39)
						79°1.90′	4°9.99′	2575	
	MSM77		S3	3-5	17/09/18	78°37.01′	5°0.04′	2313	762 (39)
						78°37.01′	5°9.60′	2300	
2019	PS121	OFOS	N3	49-1	08/09/19	79°35.89′	5°10.59′	2781	729 (40)
						79°34.08′	5°13.71′	2687	
			HG-IV	7-4	19/08/19	79°3.88′	4°17.78′	2400	834 (39)
						79°2.49′	4°8.88′	2611	
			S3	10-10	20/08/19	78°37.01′	5°9.61′	2349	613 (38)
						78°36.96′	4°54.50′	2348	
2020	MSM95	OFOBS	N3	42-1	27/09/20	79°34.15′	5°15.42′	2591	739 (31)
						79°36.00′	5°10.21′	2717	
			HG-IV	38-1	26/09/20	79°1.14′	4°6.60′	2633	658 (38)
						79°3.94′	4°18.25′	2346	
			S3	27-1	22/09/20	78°36.96′	5°8.67	2293	480 (32)
						78°37.00′	4°58.75′	2313	
2021	PS126	OFOBS	N3	27-2	20/06/21	79°34.17′	5°15.09′	2599	923 (30)
						79°36.15′	5°9.19′	2723	
			HG-IV	3-21	03/06/21	79°2.15′	4°10.26′	2557	906 (34)
						79°4.36′	4°18.78′	2294	
			S3	2-15	01/06/21	78°37.01′	5°0.01′	2312	736 (37)
						78°37.01′	5°9.62′	2296	

'stones'; stalks of unknown origin were annotated as 'stalk'; anthropogenic material was annotated as 'marine debris'.

2.4. Biogenic sediment compounds

Virtually undisturbed sediment samples were collected concurrently with the camera surveys at all stations using a video-guided multiple corer (MUC) (except 2020, where only imagery but no sediment data were available). At each station, the top 5 cm of sediment were subsampled with cut-off syringes (Ø = 1.2 cm). Three pseudo-replicate samples from different cores of the same multiple corer deployment were collected for the analyses of chloroplastic pigment equivalents (CPE, sum of all pigments, μg/ml), organic carbon content (C-org, %), and exo-enzymatic bacterial activity (FDA, nmol (ml*h)$^{-1}$). Only the top centimeter of sediment was analyzed for this study. The C-org content and total CPE of the sediment were measured as a proxy for food availability on the seafloor. The total amount of organic hydrocarbons available in the sediment was assessed by measuring the organic carbon content (C-org). CPE measurements comprised a quantification of chlorophyll *a* (Chl *a*, μg/ml), as the 'fresh' component, as well as phaeopigments (Phaeo, μg/ml), as the 'degraded' component. The fluorogenic substrate fluorescein-di-acetate (FDA) was used to measure exoenzymatic bacterial activity immediately after sampling. Details of the analyses of CPE, C-org, and FDA can be found in Schnier et al. (2023) and citations therein.

2.5. Data analysis

2.5.1. Image analysis

Taxon accumulation curves were calculated based on the cumulative seafloor area of each of the selected images from the previous step. The curves were used to identify the minimum seafloor area required to capture most of the diversity. At a sampling effort of 50 m^2, the curves for most photographic surveys showed diminishing returns in the detection of new taxa (Fig. S1). For each photographic survey, which covered approximately 150 m^2, images were randomly grouped into three subsets of roughly 50 m^2 each, creating three pseudo-replicates per photographic survey to calculate the variability within each survey. Benthic megafauna taxa and habitat features were identified and quantified using biigle.de. The density of each taxon (number of individuals per m^2) and habitat feature was then calculated by dividing the total number of individuals by the cumulative seafloor area surveyed within each pseudo-replicate.

Alongside overall megafauna density per year, densities per megafauna taxa and habitat features, taxon number (S), as the raw count of unique taxa identified, Shannon-Wiener species diversity ($\log_e$-based, Shannon and Weaver, 1963), and Pielou's evenness index (Pielou, 1966) were calculated per replicate.

For a functional trait analysis, all taxa were grouped into broad modalities of five functional traits: Feeding type including deposit feeders, suspension feeders, predator/scavengers and undefined; Mobility type including mobile taxa, sessile taxa and undefined; Zoogeography comprising cosmopolite, Arctic, Arctic-boreal and

undefined; Size class comprising small, small-medium, medium, medium-large; Substratum affinity including soft, soft/hard, hard/biological and soft/hard/biological affinity (Table S1). Information on functional traits of each taxon was extracted from the literature (Bergmann et al., 2009; Taylor et al., 2017), World Register of Marine Species (WoRMS Editorial Board, 2024), and the Arctic Traits Database (Degen and Faulwetter, 2019). Additionally, taxa without substratum affinity or size class were grouped based on observations and measurements on the images. For substratum affinity, the substratum on which each individual of a taxon was found was recorded and combined into the respective substratum affinity. If individuals occurred on, for example, soft sediments and hard substrates, substratum affinity was classified as soft/hard. For size measurements, 15 individuals per taxon were randomly selected, measured lengthwise, and grouped into size classes based on the Arctic Traits Database (Degen and Faulwetter, 2019). Morphotypes without information on feeding and mobility types inherited the same types from higher taxonomic levels. The feeding and mobility type of the sea anemone *Oceanactis bursifera* was classified according to 'purple anemone' for continuity, as this organism was previously grouped within the morphotype 'purple anemone' but was now identified as a separate species.

Finally, the megafauna densities observed within this study for the period 2016-2021 were compared to densities reported in the literature for the period 2002/2004-2015, to identify continuing temporal trends in the Arctic Ocean (Bergmann et al., 2011; Taylor et al., 2017). This time period comparison focused solely on four representative taxa with the highest degree of detectability to ensure comparability between study periods and minimize the effect of improving image resolution with time and annotator bias between studies. The detectability was assessed by the size of the organisms (excluding organisms of size 'small'), annotation consistency (e.g., excluding the gastropod *Mohnia* spp., as shells could not always be distinguished from living organisms), and a total density over both periods of >1 individual m^{-2} at any of the stations. Organisms best matching those criteria were: the crinoid *Bathycrinus* cf. *carpenterii*, the soft coral *Gersemia fruticosa,* and the sea anemone morphotype 'purple actiniaria' representing important suspension feeders within the community, and the sea cucumber *Kolga hyalina* representing deposit feeders. For this comparison, *Oceanactis bursifera* was grouped under the 'purple actiniaria' morphotype to maintain consistency with data collected prior to 2016. The density data per taxon for the time period before 2016 were extracted from Bergmann et al. (2011) for HG-IV and Taylor et al. (2017) for N3 and S3. It should be noted that the calculations of mean densities followed two different schemes and were based on different seafloor coverages for the two time periods. For the time period before 2016, mean densities were calculated by averaging the densities observed on each image within a photographic survey. The image number and investigated seafloor area varied by station: at HG-IV, seafloor coverage ranged from 101 to 171 m^2 (40 images; Bergmann et al., 2011), at N3, from 305 to 320 m^2 (80 images; Taylor et al., 2017), and at S3 from 265 to 325 m^2 (40-80 images; Taylor et al., 2017). For the time period from 2016 onwards, mean densities were calculated by averaging over the three replicates, each with approx. 50 m^2 seafloor coverage and thus 150 m^2 investigated seafloor area per year and station. Despite these differences, we believe that the final numbers are comparable by acknowledging the constraints during the interpretation process.

2.5.2. Statistical analysis

To test for community differences across stations and years within each station, various analyses were conducted on a Bray-Curtis similarity matrix based on square-root transformed density data to correct for the inflated effect of very abundant taxa. Similarities between stations and years were depicted in a non-metric multidimensional scaling (nMDS) plot, with stress values indicating the accuracy of the two-dimensional representation (Clarke, 1993). Using the dissimilarity matrix, Shepard plots were inspected to confirm the relationship between the original dissimilarities and ordination distances. The depicted community differences were tested with a one-way analysis of similarity (ANOSIM, Clarke, 1993). The ANOSIM procedure was run once per station and once per combination of years. This was followed by a similarity percentages procedure (SIMPER, Clarke, 1993) to identify discriminating taxa that contributed to at least 70% of the differences between years. The relationship between environmental variables and community variation was investigated by distance-based redundancy analysis (db-RDA, Legendre and Anderson, 1999), an ordination method that allows for non-Euclidean dissimilarity indices. The db-RDA was run on a Bray-Curtis similarity matrix based on square-root transformed density data. The year 2020 was excluded from the analysis, as sediment parameters were not available for this year. Correlation tests were performed for pairwise correlation between environmental variables. A high correlation coefficient ($|r| > 0.95$, Anderson et al., 2008) resulted in the exclusion of variables. The constrained ordination was tested with permutation tests to identify the significance of the model and the influence of environmental variables. Only variables with significant influence ($p < 0.005$) were selected and used to re-run the reduced db-RDA model and to generate ordination plots. The relative importance of each set of variables explaining community variation was investigated by variation partitioning based on the db-RDA model using adjusted R-squared as a criterion to assess the partitions (Legendre and Anderson, 1999; McArdle and Anderson, 2001). Permutation tests on the individual fractions of each environmental variable to test the significance of each fraction followed.

All statistical analyses were done in R (v4.4.1, R Core Team, 2024) using the packages "tidyr" (v1.3.1, Wickham et al., 2024) and "dplyr" (v1.1.4, Wickham et al., 2023) for dataset restructuring, "vegan" (v2.6-6.1, Oksanen et al., 2022), "FD" (v1.0-12.3, Laliberte et al., 2014) and "rstatix" (v0.7.2, Kassambara, 2023a) for the data analysis and "ggplot2" (v3.5.1, Wickham, 2016), "ggpubr" (v0.6.0, Kassambara, 2023b), "ggtext" (v0.1.2, Wilke and Wiernik, 2022), "markdown" (v2.0, Xie et al., 2025), "scales" (v1.4.0, Wickham et al., 2025) and "patchwork" (v1.3.2, Pedersen, 2025) to generate plots.

3. Results

3.1. Taxon inventory

A total of 33 taxa and morphotypes were annotated across all stations and years (Fig. 2). Of the total number, 20 taxa were identified to species level: *Ascorhynchus abyssi, Catherinum striolatum, Bathycrinus* cf. *carpenterii, Bylgides groenlandicus, Caulophacus arcticus, Cladorhiza gelida, Colossendeis proboscidea, Poliometra prolixa, Elpidia heckeri, Gersemia fruticosa, Halirages cainae, Hymenaster pellucidus, Oceanactis bursifera, Kolga hyalina, Lissodendoryx complicata, Lycodes frigidus, Neohela lamia, Pourtalesia jeffreysi, Saduria megalura,* and cf. *Bathyphellia margaritacea*. Three taxa were identified to genus level (*Amphianthus* sp., *Bythocaris* spp., *Mohnia* spp.), one taxon to class level (Bivalvia), and nine morphotypes were classified ('small isopod', 'long-tentacled actiniaria', 'narrow white sponge', 'purple actiniaria', 'small round sponge', 'white long-tentacled actiniaria', 'white crustacea', 'small sponge on hard substrate', and 'tube-dwelling polychaeta').

Differences in taxon inventories among the three stations were evident for eight taxa. The following four taxa were frequently observed at HG-IV and S3 but were absent from N3: *Gersemia fruticosa, Neohela lamia, Saduria megalura,* and 'white long-tentacled actiniaria'. Three taxa were observed at N3 and HG-IV, but absent from S3: *Kolga hyalina, Lissodendoryx complicata,* and 'narrow white sponge'. The morphotype 'long-tentacled actiniaria' was exclusively present at HG-IV.

3.2. Short-term variability of megafauna community composition

We analyzed taxonomic and functional community composition of the benthic megafauna across three stations located within the

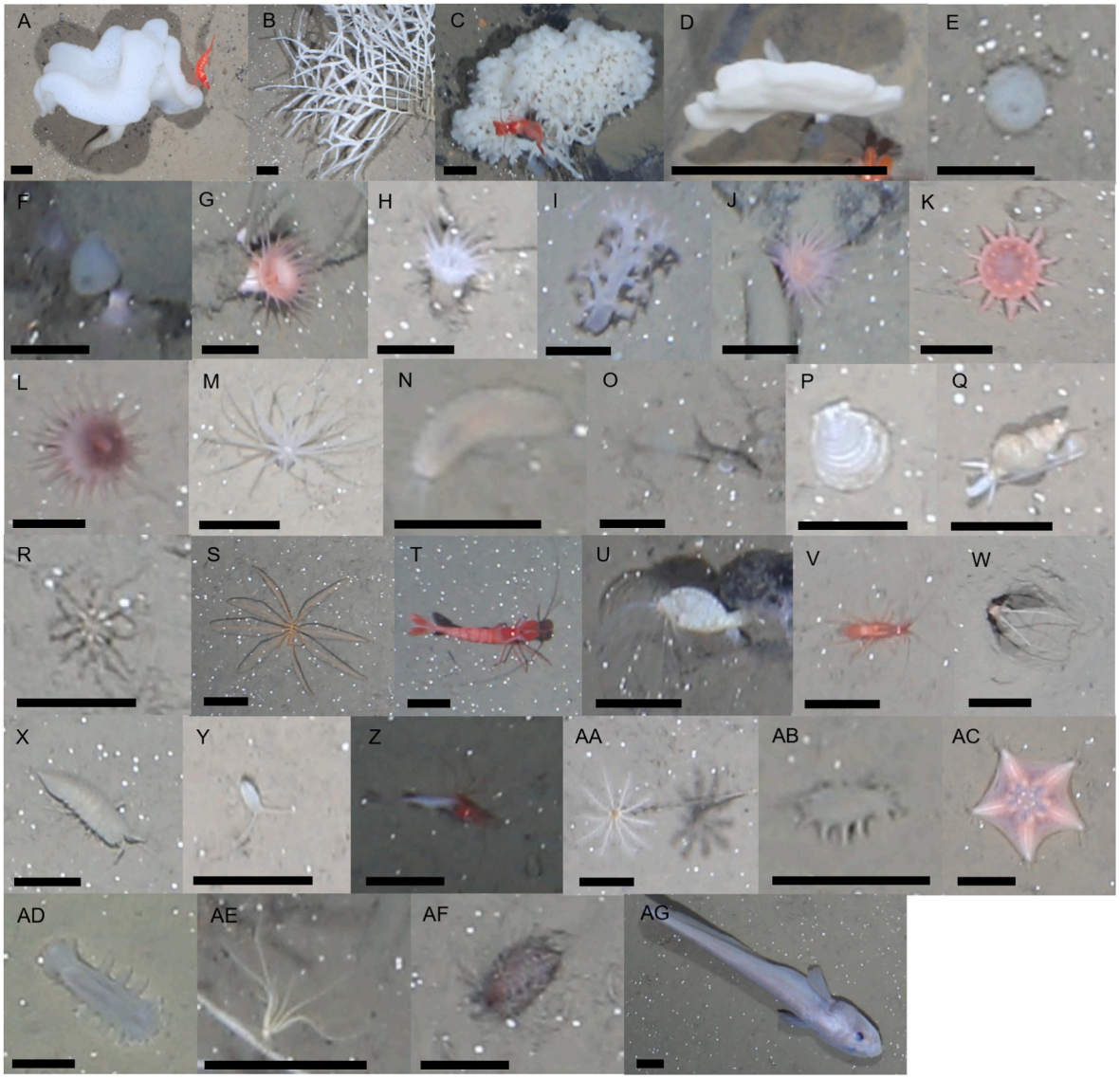

Fig. 2. Example images of taxa/morphotypes of benthic megafauna observed during photographic surveys at the HAUSGARTEN stations N3, HG-IV, and S3. (A) *Caulophacus arcticus*, (B) *Cladorhiza gelida*, (C) *Lissodendoryx complicata*, (D) narrow white sponge, (E) small round sponge, (F) small sponge hard substrate, (G) *Amphianthus* sp., (H) cf. *Bathyphellia margaritacea*, (I) *Gersemia fruticosa*, (J) long-tentacled actiniaria, (K) *Oceanactis bursifera*, (L) purple actiniaria, (M) white long-tentacled actiniaria, (N) *Bylgides groenlandicus*, (O) tube-dwelling polychaeta, (P) Bivalvia, (Q) *Mohnia* spp., (R) *Ascorhynchus abyssi*, (S) *Colossendeis proboscidea,* (T) *Bythocaris* spp., (U) *Catherinum striolatum*, (V) *Halirages cainae*, (W) *Neohela lamia*, (X) *Saduria megalura*, (Y) small isopod, (Z) white crustacea, (AA) *Bathycrinus* cf. *carpenterii*, (AB) *Elpidia heckeri*, (AC) *Hymenaster pellucidus*, (AD) *Kolga hyalina*, (AE) *Poliometra prolixa*, (AF) *Pourtalesia jeffreysi*, (AG) *Lycodes frigidus*. Black bars indicate 2.5 cm.

HAUSGARTEN observatory over a six-year period. The benthic megafauna community fluctuated in overall densities at all three stations. The highest overall density at N3 was observed in 2019 with 16.2 ± 1.8 ind. m^{-2} (Fig. 3 N3). The lowest density was observed one year before in 2018 with 8.8 ± 0.1 ind. m^{-2}, resulting in an 85% increase from 2018 to 2019. The density decreased again in the following year by 32%. At HG-IV, the density increased by 25% from 2018 to the highest density in 2019 with 11.6 ± 0.4 ind. m^{-2}, and decreased by 20% in 2020 (Fig. 3 HG-IV). The lowest density was observed in 2021 with 5.5 ± 0.5 ind. m^{-2}, a 41% decrease from the previous year. The megafauna densities at the southernmost station, S3, were highest in 2017, at 14.2 ± 0.4 ind. m^{-2}, following a 62% increase from 2016. This was followed by a 42% decrease in 2018 (Fig. 3 S3). The second-highest density was observed in 2019 with 9.9 ± 0.4 ind. $m^{-2,}$ suggesting a station-wide pattern of increased densities in 2019 compared to 2018. The lowest density at S3 was found in 2020 with 4.8 ± 0.5 ind. m^{-2}, a decrease of 51% from the previous year. Abundance data are provided in Tables S2–S4 of Supplementary Materials I for N3, HG-IV, and S3, respectively.

Interannual differences were also found for the diversity indices (Fig. 4). The highest taxon number (S) was recorded in 2016 for N3 with a mean of 18.3 taxa, in 2020 for HG-IV with a mean value of 19.7, and in 2016 for S3 with 21 taxa. The lowest S was recorded in 2021 at N3 with 14.3, in 2018 and 2019 at HG-IV with 14.7, respectively, and in 2020 at S3 with 17.7 taxa. Shannon-Wiener diversity H′ and Pielou's Evenness J′ also varied over time at all stations. At N3, H′ and J′ decreased continuously from 2016 to 2020, with 2.3 to 1.6 for H′ and with 0.8 to 0.5 for J'. At HG-IV, H′ and J′ decreased from 2016 to their lowest values in 2019, with 2.0 to 1.5 and 0.7 to 0.6 for J'. Both indices increased in the following years, with the highest values in 2021 (H': 2.1; J': 0.7). At S3, the lowest H′ and J′ were recorded in 2017, with 1.7 H′ and 0.6 J'. Both indices showed higher values in the following years again.

The clustering of replicates and the formation of distinct groups for

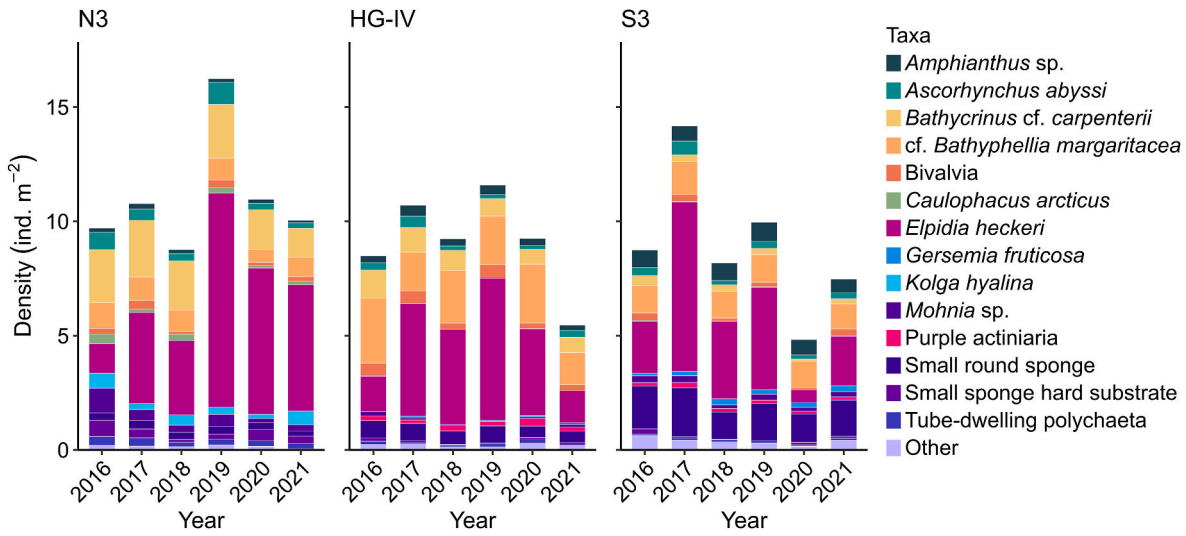

Fig. 3. Mean density of benthic megafauna organisms (ind. m^{-2}) of stations N3, HG-IV, and S3 in the HAUSGARTEN observatory, Arctic Ocean. Different colors represent taxa with >2 ind. m^{-2} at any station. Remaining taxa are grouped in 'Other'. N = 3.

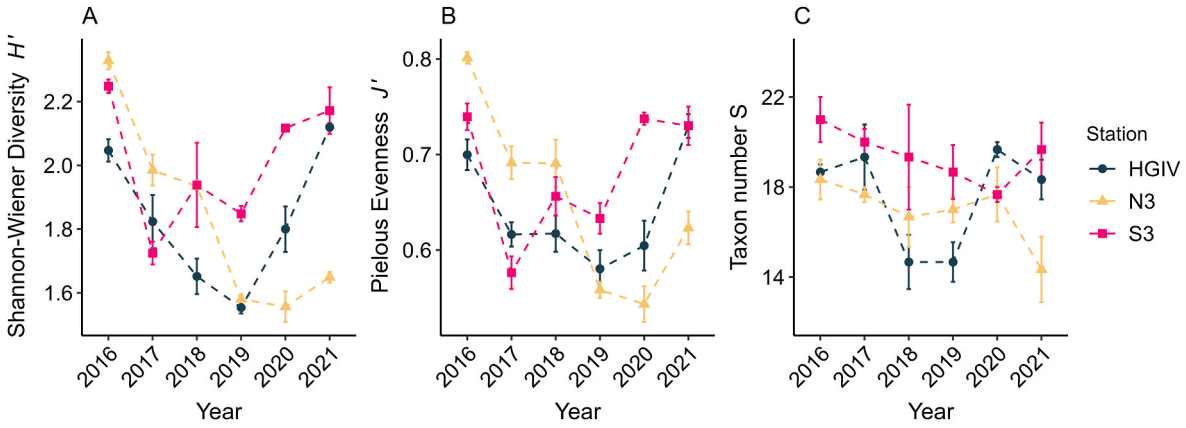

Fig. 4. Diversity indices of the benthic megafauna community of stations N3, HG-IV, and S3 in the HAUSGARTEN observatory, Arctic Ocean. (A) Shannon-Wiener diversity index ($\log_e$-based) *H'*; (B) Pielou's Evenness index *J'*; (C) Taxon number S. Colors and shapes represent different stations. Point shapes indicate the mean; solid horizontal lines indicate the standard error of the mean. N = 3.

most years on the nMDS plots (Fig. 5) revealed pronounced differences in megafauna community composition at each station. Temporal trajectories reveal a consistent shift in community structure over time. This pattern is supported by the global ANOSIM tests, which yielded high R-values and significant p-values at each station (Table 2). However, due to the limited sample size (n = 3) and the consequently restricted number of permutations for pairwise ANOSIM comparisons, none of the pairwise tests reached statistical significance. Despite this limitation, R-values exceeding 0.8 can still be interpreted as evidence of strong ecological differences between communities (Clarke and Warwick, 2001), as the pairwise ANOSM tests failed to reach significance due to small sample sizes rather than a true absence of effects, as demonstrated at station N3. At the other two stations, most pairwise comparisons also showed high R-values, with exceptions at HG-IV for the period 2018 to

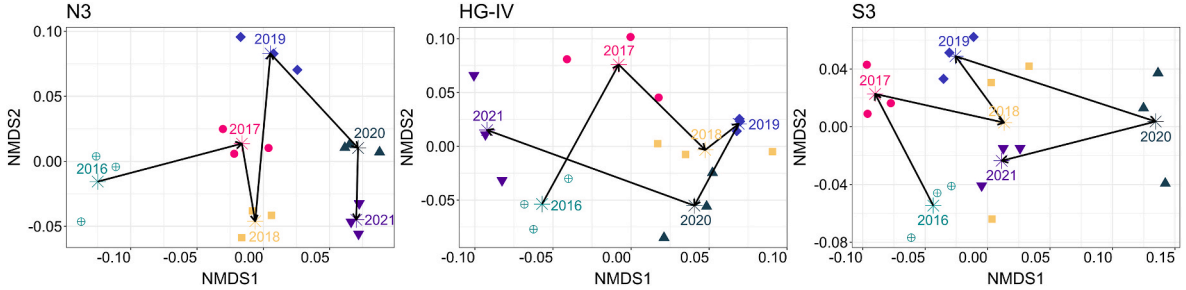

Fig. 5. nMDS plots depicting the dissimilarity in community structure from 2016 to 2021 at stations N3, HG-IV, and S3 in the HAUSGARTEN observatory, Arctic Ocean. Colors and shapes represent different years. Centroids were calculated per year and depicted as stars. Temporal trajectories indicate the direction of the shift in community composition. Two-dimensional stress at N3: 0.106, at HG-IV: 0.175, and at S3: 0.134. N = 3.

Table 2
ANOSIM community structure (R) and p-values (p) on Bray-Curtis similarity matrix based on square-root transformed density data.

Years compared	N3		HG-IV		S3	
	R	p	R	p	R	p
2016 – 2017	1	0.1	1	0.1	1	0.1
2016 – 2018	1	0.1	1	0.1	0.70	0.1
2016 – 2019	1	0.1	1	0.1	1	0.1
2016 – 2020	1	0.1	1	0.1	1	0.1
2016 – 2021	1	0.1	0.74	0.1	0.63	0.1
2017 – 2018	1	0.1	0.67	0.1	0.78	0.1
2017 - 2019	1	0.1	0.74	0.1	0.78	0.1
2017 – 2020	0.96	0.1	1	0.1	1	0.1
2017 – 2021	1	0.1	0.85	0.1	1	0.1
2018 – 2019	1	0.1	0.96	0.1	0.26	0.2
2018 – 2020	1	0.1	0.41	0.2	1	0.1
2018 – 2021	1	0.1	0.96	0.1	0.48	0.2
2019 – 2020	1	0.1	0.78	0.1	1	0.1
2019 – 2021	1	0.1	1	0.1	0.96	0.1
2020 – 2021	0.96	0.1	1	0.1	1	0.1
Global	0.99	0.001	0.81	0.001	0.78	0.001

2020 (R = 0.41), and at S3 for 2018 to 2019 (R = 0.26) and 2018 to 2021 (R = 0.48). Notably, the year 2018 at both stations displayed a wider dispersion compared to other years.

The SIMPER analysis revealed that the small sea cucumber *Elpidia heckeri* contributed the most to the average between-group dissimilarity across all stations (average contribution to the overall dissimilarity: 21% at N3 and S3 and 16% at HG-IV). The densities of *E. heckeri* generally followed the same trend as the overall megafauna densities for all stations (see Fig. 3). At N3, the highest density was observed in 2019 (9.4 ± 1.2 ind. m^{-2}), and the lowest density in 2016 (1.3 ± 0.1 ind. m^{-2}). The highest *E. heckeri* density at HG-IV was found in 2019 (6.2 ± 0.1 ind. m^{-2}). At S3, the highest density was found in 2017 (7.4 ± 0.3 ind. m^{-2}) and the lowest in 2020 (0.5 ± 0.1 ind. m^{-2}). The taxon with the second-highest, though considerably smaller, average contribution to overall community dissimilarity varied by station: *Mohnia* spp. accounted for 7% at N3, cf. *Bathyphellia margaritacea* contributed 6% at HG-IV, and 'small sponge hard substrate' represented 6% at S3.

Dominant functional traits also varied interannually (Fig. 6). In the first study year, 2016, the megafauna communities at all stations were characterized by suspension feeders. Their proportions amounted to 60% at N3, 73% at HG-IV, and 60% at S3 of the total megafauna community. In the following years, the proportions of deposit feeders increased. For N3, deposit feeders increased until 2021 when they made up 61% of the community. For HG-IV, the highest proportion of deposit feeders was found in 2019 (54%) and decreased thereafter. For S3, the highest proportion of deposit feeders was found in 2017 (54%), and in 2020, suspension feeders re-dominated the community with a proportion of 79%, whereas deposit feeders only made up 13% of the total community. A similar trend could be observed for mobility types, zoogeography, and substrate affinity, where the proportions of megafauna represented by mobile, Arctic-boreal taxa with soft substratum affinity almost steadily increased, and the proportion of sessile, Arctic taxa with a soft/hard substratum affinity declined from 2016 to 2019 for N3 and HG-IV. For S3, the highest proportion of Arctic-boreal taxa was observed in 2017 (59%) and the lowest in 2020 (21%). In the same year, 2020, the highest proportions of Arctic (32%) and cosmopolitan (14%) taxa were recorded. By contrast, variations in dominant size classes were low. 'Small-medium' taxa dominated the community at all stations and years, but represented fluctuating proportions of the station total densities, never falling below 70%. At S3, 'small' taxa accounted for higher proportions compared to the other stations, but never exceeded 30%.

3.3. Environmental variables

Each station was characterized by a certain combination of habitat features across the analyzed images, with particularly structural components varying in proportion and density over time (Fig. 7). At the station N3, the highest densities were of 'shell', 'sponge debris', and 'stone'. The highest number of total habitat features at this station was observed in 2016 and 2019 (3.2 ± 0.1 and 3.2 ± 0.2 features m^{-2}, respectively). Lowest total habitat features were observed in 2020 (1.3 ± 0.2 features m^{-2}). At HG-IV, the habitat was also characterized by high densities of 'shell'. The highest density of total habitat features at this station was found in 2016 (2.1 ± 0.2 features m^{-2}), and the lowest density was recorded in 2018 (1.0 ± 0.2 features m^{-2}). The habitat at S3 was primarily characterized by 'burrows', which were the habitat feature with the highest density in all years at this station. The highest total habitat feature density was found in 2016 (2.1 ± 0.3 features m^{-2}), and the lowest was recorded in 2020 (1.1 ± 0.1 features m^{-2}). Abundance data of habitat features are provided in Tables S2–S4 of Supplementary Materials I for N3, HG-IV, and S3, respectively.

The concentration of biogenic sediment compounds varied across stations and years (Fig. 8). The organic carbon content was highest in 2019 for N3 and HG-IV (0.93 ± 0.11% and 0.75 ± 0.05%), and in 2016 for S3 (0.89 ± 0.09%). The lowest values were found in 2017 for N3 (0.78 ± 0.03%), in 2021 for HG-IV (0.61 ± 0.11%), and in 2018 for S3 (0.62 ± 0.13%). The bacterial activity (FDA) was highest in 2018 for N3 (10.03 ± 2.38 nmol (ml*h)$^{-1}$) and HG-IV (7.26 ± 1.24 nmol (ml*h)$^{-1}$), and in 2017 for S3 (6.49 ± 2.10 nmol (ml*h)$^{-1}$). At N3, the lowest values were measured in 2019 (1.37 ± 0.45 nmol (ml*h)$^{-1}$), at HG-IV in 2021 (1.43 ± 0.16 nmol (ml*h)$^{-1}$), and at S3 in 2019 (2.60 ± 0.52 nmol (ml*h)$^{-1}$). The 'fresh' phytodetrital matter, chlorophyll *a* (Chl *a*), peaked in 2018 for N3 (8.35 ± 4.93 μg/ml), in 2021 for HG-IV (5.71 ± 0.24 μg/ml), and in 2021 for S3 (5.22 ± 0.69 μg/ml). Chl *a* was lowest in 2017 for N3 (1.61 ± 0.29 μg/ml) and HG-IV (1.93 ± 0.37 μg/ml), and in 2018 for S3 (1.38 ± 0.47 μg/ml). Peak values of 'degraded' phytodetrital matter, phaeopigments (Phaeo), were measured in 2019 for N3 (26.76 ± 0.96 μg/ml), in 2021 for HG-IV (33.01 ± 13.31 μg/ml), and in 2021 for S3 (32.27 ± 2.72 μg/ml). Lowest values were found in 2018 for N3 (14.94 ± 4.11 μg/ml), in 2017 for HG-IV (16.01 ± 3.98 μg/ml), and in 2016 for S3 (17.08 ± 2.15 μg/ml). Values per station and years are provided in Table S5 of Supplementary Materials I.

3.4. Influence of environmental variables on megafauna community composition

There was no collinearity between environmental variables. The first permutation test on the db-RDA model was significant (df = 18, F = 11.4, p = 0.001) but revealed non-significant (p > 0.005) influences of four variables (phaeopigments, FDA, 'echinoid test', and 'stalk'). Variables showing non-significant effects were excluded from subsequent analyses, and a reduced model was constructed using the remaining variables. Permutation tests on this reduced model confirmed significant influences of environmental variables on megafauna community composition (df = 14, F = 12.8, p = 0.001), with each individual variable also showing significance (p < 0.005). Although the adjusted R-squared of the reduced model (0.79) was slightly lower than that of the full model (0.81), we chose the reduced model due to the non-significance of excluded variables and improved interpretability of the main drivers. The retained environmental variables explained 86% of the variation in community composition. Within the dbRDA ordination, the first two axes accounted for 72% (dbRDA1) and 24% (dbRDA2) of the variation explained by the model (Fig. 9). Station separation was observed along the x-axis, driven mainly by habitat features. Specifically, 'burrow' showed a positive association with station S3, while all other habitat features were positively correlated with station N3. The y-axis captured both temporal variation within each station and the distinct separation of station HG-IV. This suggests that unaccounted environmental variables, associated with the y-axis, drove the unique community structure observed at HG-IV.

The results of the variation partitioning of the megafauna

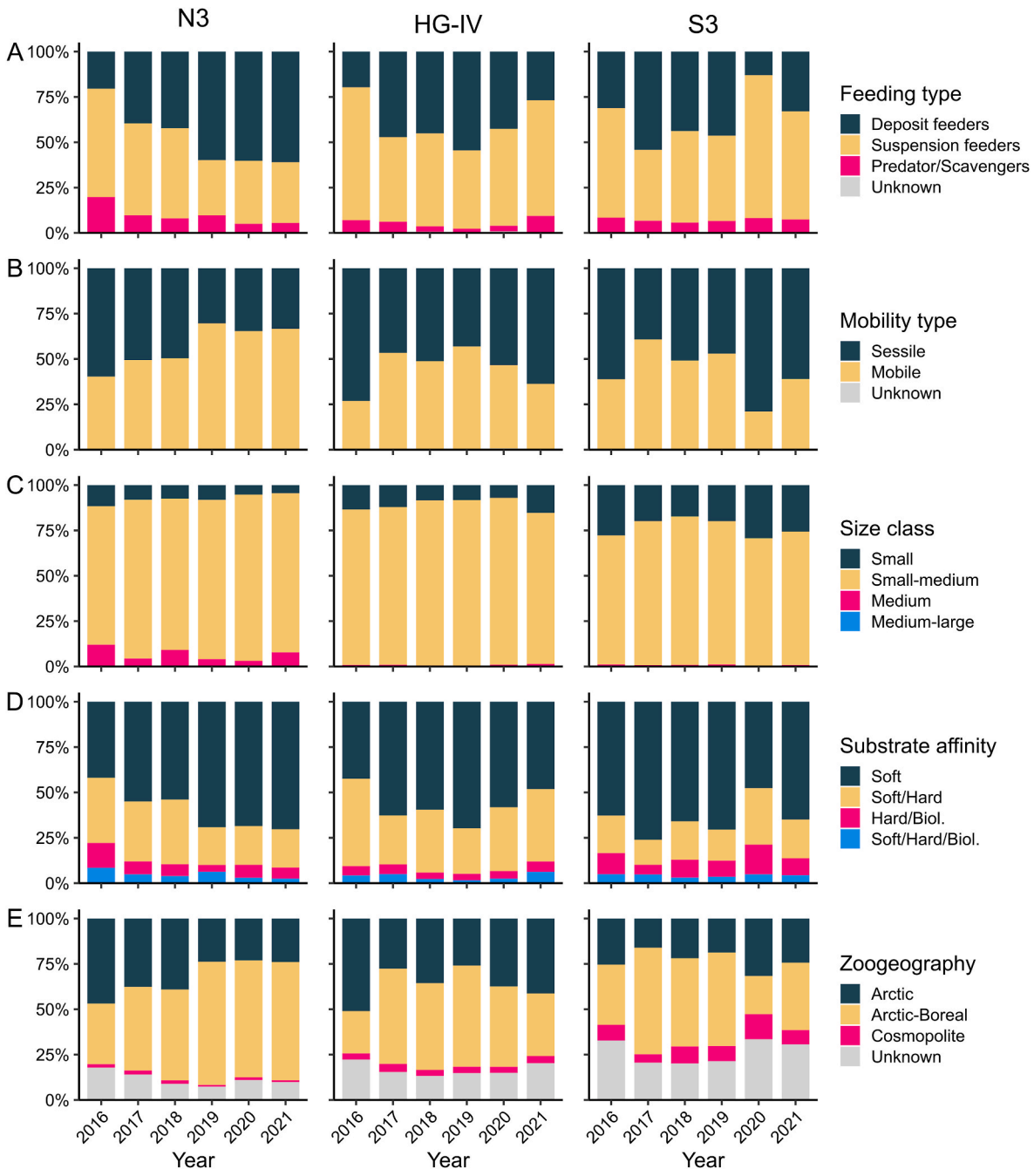

Fig. 6. Proportion of different modalities of functional traits of the benthic megafauna community at stations N3, HG-IV, and S3 in the HAUSGARTEN observatory, Arctic Ocean. (A) Feeding type; (B) Mobility type; (C) Size class; (D) Substratum affinity (biol. = biological); (E) Zoogeography. N = 3.

community variation are shown in Fig. 10. The highest shared fraction of explained community variation was found for the intersection of habitat features and station, with 42%. The second-highest shared fraction was found for the intersection of habitat features, station, and sediment parameters, explaining 12% of the variation. The cumulative fraction, i.e., including all shared fractions, explained by station was 59%, by habitat features 57%, by biogenic sediment compounds 11%, and by years 8% of the community variation. Individual fractions, i.e., fractions of variation explained by each set of environmental variables excluding all shared fractions, were considerably lower and explained between 1 and 10% of the variation with biogenic sediment compounds, habitat features, station, and year in increasing order. The percentage of unexplained variation was 21%.

Permutation tests of individual fractions revealed insignificant effects of biogenic sediment compounds on the community variation ($df = 2$, $F = 1.53$, $p = 0.139$). The effect of habitat features was significant ($df = 6$, $F = 2.79$, $p = 0.001$) with 'stone' as the only significant factor ($p < 0.005$). Individual fractions of year and station were also significant (year, $df = 4$, $F = 5.13$, $p = 0.001$; station, $df = 2$, $F = 8.31$, $p = 0.001$).

3.5. Long-term variability in density of selected taxa

All selected taxa, including the crinoid *Bathycrinus* cf. *carpenterii*, the soft coral *Gersemia fruticosa*, the sea cucumber *Kolga hyalina*, and the sea anemone morphotype 'purple actiniaria', exhibited higher densities during the first period (2002/2004 to 2015) compared to the second period (2016 to 2021) (Fig. 11). At station N3, the soft coral and sea anemone were absent after 2004. The densities of the crinoid and sea

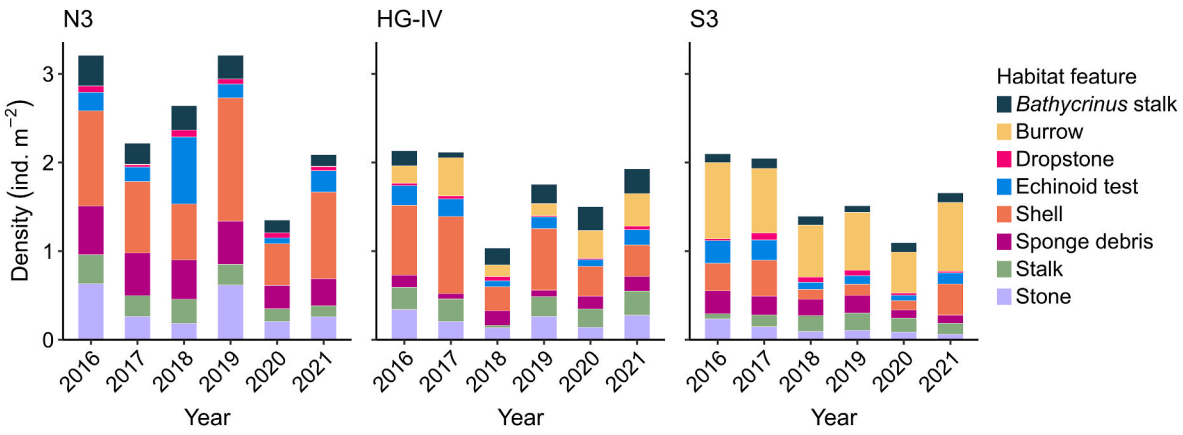

Fig. 7. Composition of most abundant habitat features (ind. m^{-2}) at N3, HG-IV, and S3 in the HAUSGARTEN observatory from 2016 to 2021. N = 3.

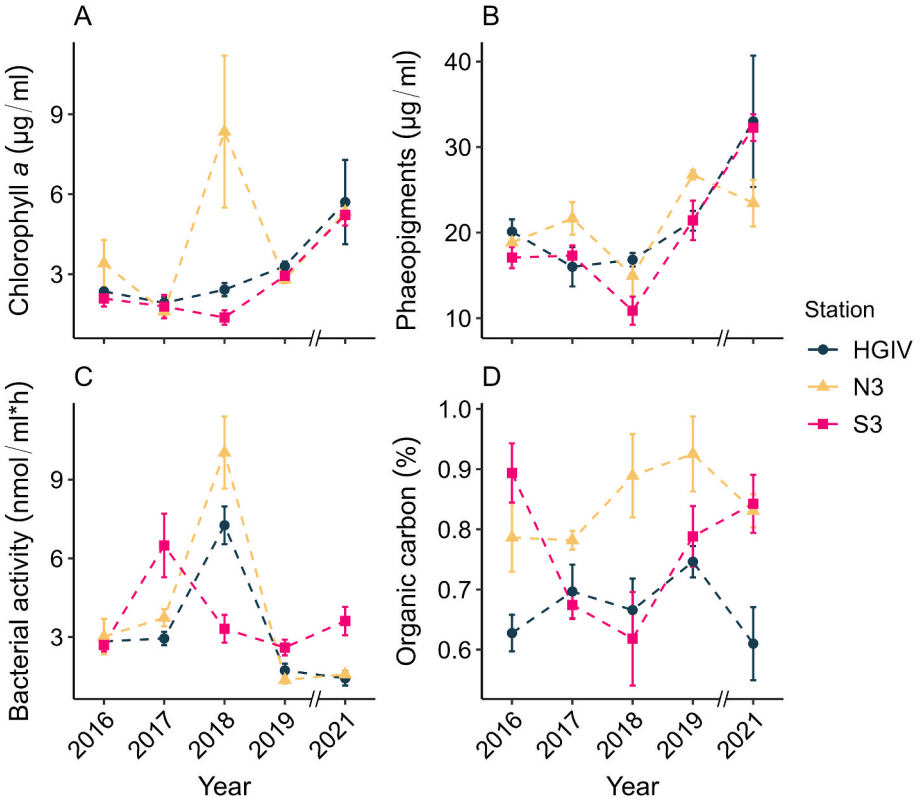

Fig. 8. Biogenic sediment compounds measured at N3, HG-IV, and S3 from 2016 to 2021 for (A) chlorophyll *a*, (B) phaeopigments, (C) bacterial activity, and (D) organic carbon. Colors and shapes represent different stations. Vertical lines indicate the standard error of the mean. The broken x-axis indicates non-continuity due to the lack of data in 2020. N = 3.

cucumber declined almost continuously over time, with the sea cucumber showing a rapid decrease from 2007 to 2020, resulting in an 84% reduction in mean density between the two periods. The crinoid density declined by 28% between these study intervals. At HG-IV, the crinoid, sea anemone, and soft coral exhibited similar temporal patterns in their densities. High densities recorded in 2002 and 2007 were followed by a substantial decline by 2016. Density reductions between the two periods were 61% for the crinoid, 93% for the soft coral, and 76% for the sea anemone. The sea cucumber was largely absent at HG-IV, appearing only sporadically. At station S3, densities of all selected taxa were considerably lower (<1 individual m^{-2}) compared to the other stations. Nonetheless, the same trend of higher densities during the first period (before 2016) was evident, with reductions of 60% for the crinoid, 58% for the soft coral, and 35% for the sea anemone. The sea cucumber was also mostly absent at S3.

4. Discussion

Given that climate change in the Arctic is progressing four times faster than the global average (Rantanen et al., 2022), it is important to investigate and monitor how this affects ecosystem dynamics, including benthic community composition. Time-series studies are a valuable tool for monitoring changes in benthic communities, particularly in understudied regions such as the Arctic Ocean. Previous research has shown that benthic communities are highly dynamic and exhibit variable responses to changing environmental conditions (Bergmann et al., 2011; Górska et al., 2022; Meyer-Kaiser et al., 2025; Taylor et al., 2017). While variation in megafaunal densities is generally linked to sediment

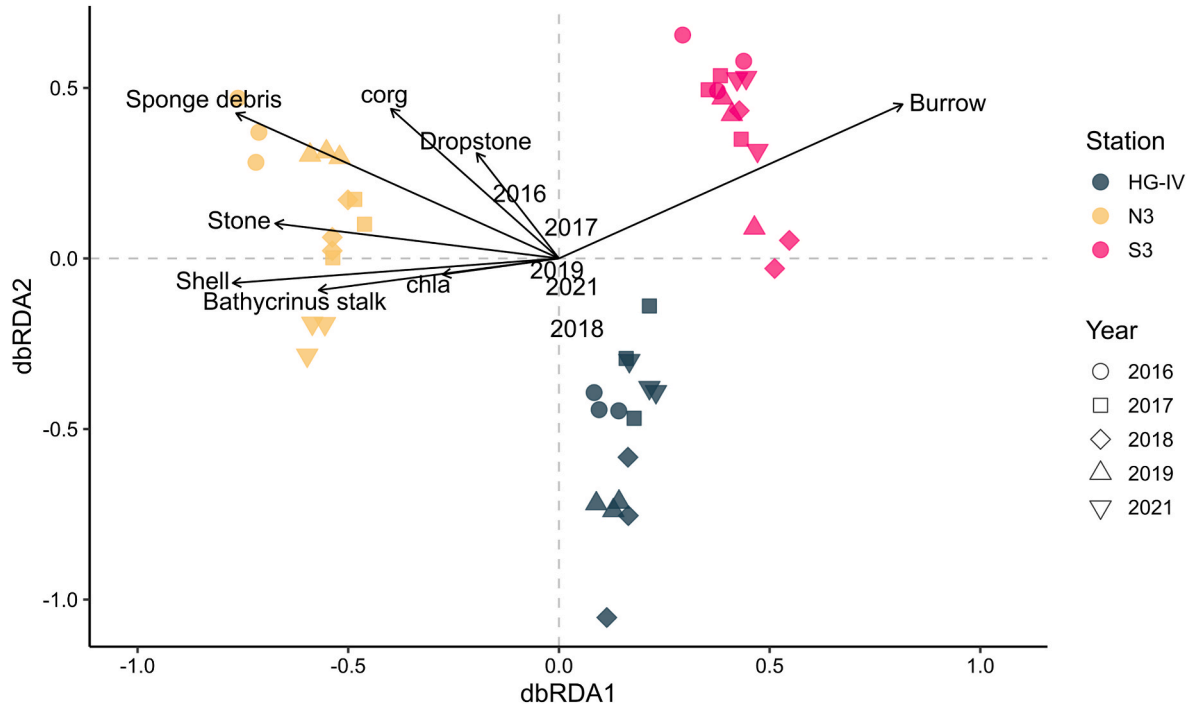

Fig. 9. Biplot of the distance-based redundancy analysis (db-RDA) result illustrating the relationship between environmental variables and community variation. The db-RDA was performed on Bray-Curtis similarity matrix based on square-root transformed density data. 'chla' = Chlorophyll *a*; 'corg' = organic carbon. Colors represent each station (HG-IV: dark teal; N3: yellow; S3: pink), and shapes represent each year. The year 2020 was excluded from the analysis because data on biogenic sediment compounds were unavailable.

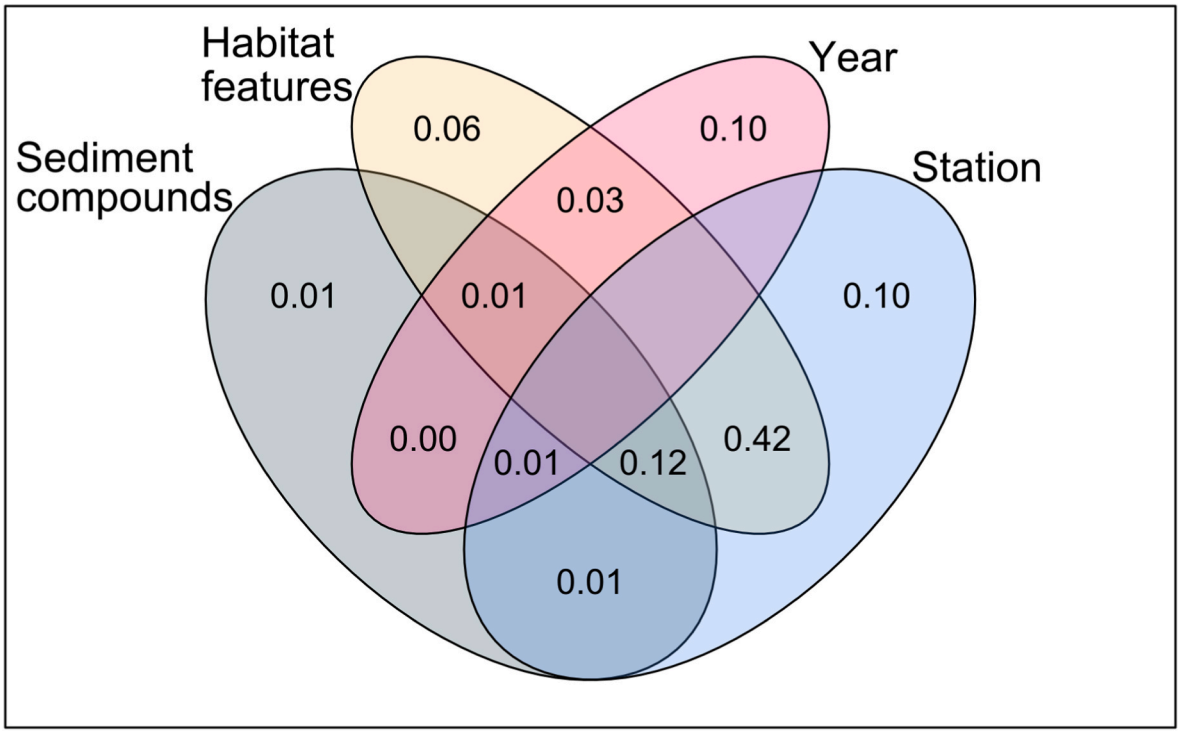

Fig. 10. Venn diagram representing the partition of the variation of benthic megafauna community composition between four sets of explanatory variables with biogenic sediment compounds (sediment compounds), habitat features, year, and station. The non-overlapping areas show the unique contribution of each variable. The overlapping areas represent the shared variation. Residuals = 0.21. Values < 0 not shown.

parameters related to food availability (Bergmann et al., 2011; Meyer et al., 2013), Taylor et al. (2017) found that megafauna densities increased alongside higher habitat heterogeneity, specifically through greater dropstone density, a pattern that was also found on the east Greenland slope (Schulz et al., 2010). To further elucidate these dynamics, we investigated the benthic megafauna community composition

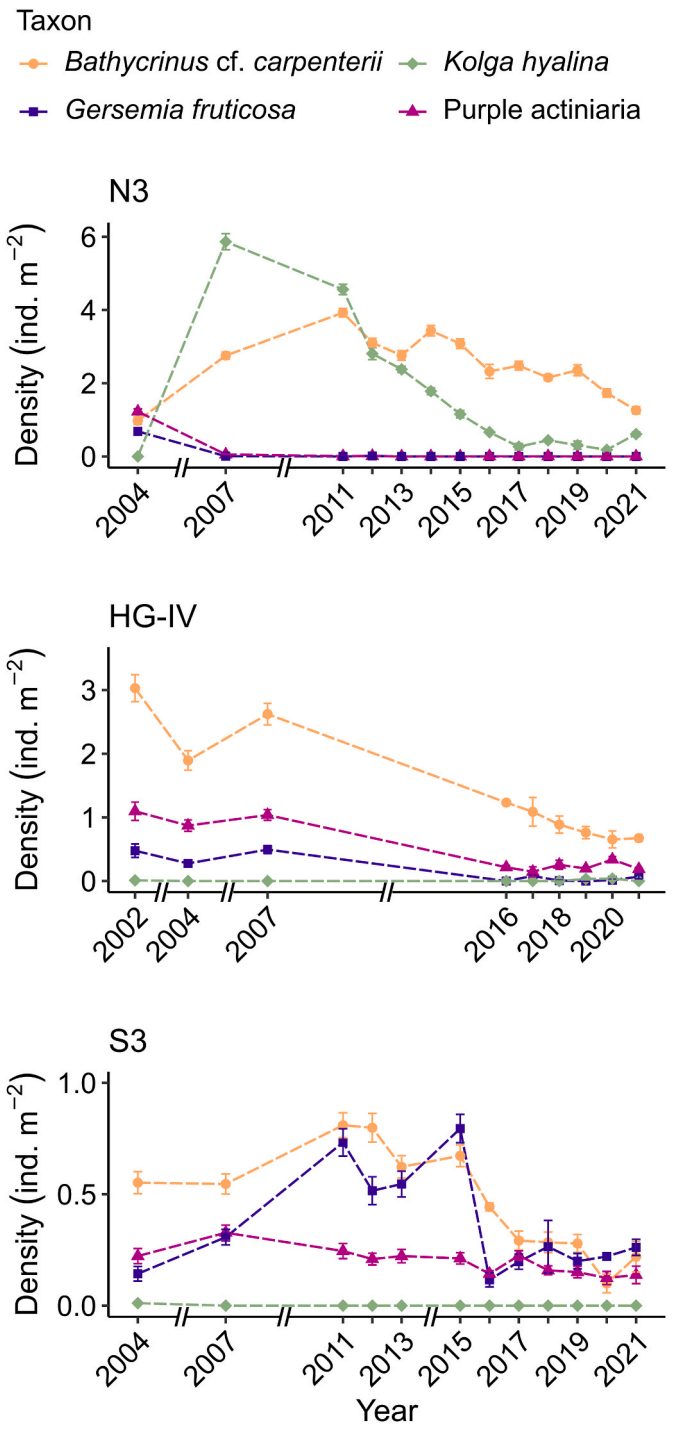

Fig. 11. Long-term variability in density of four selected taxa at three stations (N3, HG-IV, S3) of the HAUSGARTEN observatory. Different colors and shapes represent different taxa. Point shapes indicate the mean; vertical lines indicate the standard error of the mean. The broken x-axis indicates non-continuity due to the lack of data in certain years. Data from 2002/2004 to 2015 were extracted from Taylor et al. (2017) for N3 and S3, and Bergmann et al. (2011) for HG-IV. Data from 2016 to 2021 were reported within this study. Abundance data from before 2016 represent a mean across all images (N = 40-80). Data from after 2016 was averaged over three randomly generated replicates (N = 3).

at three stations (N3, HG-IV, and S3) within the HAUSGARTEN observatory regarding the short-term variability in taxonomic and functional composition from 2016 to 2021, in relation to environmental parameters and long-term variability by selection of four representative taxa as a continuation of the time-series started in 2002.

4.1. *Short-term variability of benthic megafauna community composition*

Over a period of six years, the benthic megafauna community composition showed strong temporal variability at all three stations of the HAUSGARTEN observatory investigated. For each year, distinct communities were observed, with temporal trajectories showing a consistent shift over time, indicating temporally changing communities and succession in community composition at each station. However, the SIMPER analysis revealed specifically one taxon to be the main contributor to interannual differences at all stations. This was corroborated by years with high overall density being coupled with low diversity and evenness, suggesting that community changes were driven by density fluctuations of a few selected taxa, rather than taxon number. In our case, the taxon with the highest contribution to differences between years was the small sea cucumber *Elpidia heckeri*. This species showed highly fluctuating densities for each year at all three stations. For the years leading up to 2016, the same species was identified to be one of the main contributors to interannual differences and showed similar drastic changes in density (Taylor et al., 2017). Rapid increases from one year to the next in *E. heckeri* population density may be explained by its opportunistic feeding behavior (Bluhm et al., 2011) and ability to time its spawning according to favorable environmental conditions (Kremenetskaia et al., 2020). Additionally, congeners of Elpidiidae have been observed to undergo pronounced 'boom-bust' cycles in response to food availability with large interannual variations in density (Billett et al., 2010; Kuhnz et al., 2014). Not only recruitment, but also migration from adjacent areas could increase holothurian density, as reported for various megafauna species at the shallower HAUSGARTEN station HG-I (Meyer et al., 2013). However, it has been noted that increases in holothurian density are often correlated with decreases in size and biomass (Ruhl, 2007; Taylor et al., 2018), suggesting that recruitment rather than migration is more likely to be responsible for increases in density.

Variability in functional community composition was evident at all three HAUSGARTEN stations over the six-year period. Given the strong influence of *E. heckeri* density on overall megafauna abundance, it is expected that functional traits also varied alongside changes in this small sea cucumber's density. While the intrinsic characteristics of *E. heckeri* partly explain its success in certain years, examining its functional role offers deeper insight into the drivers of community shifts. In years of high *E. heckeri* density (i.e., 2016 for all stations, 2021 for HG-IV, and 2020 for S3), the community was dominated by deposit-feeding, mobile organisms that prefer soft substrates and exhibit an Arctic-boreal distribution. *E. heckeri* itself exemplifies this group. In contrast, years with low *E. heckeri* density were characterized by larger proportions of suspension feeders that are mostly sessile, favor soft or mixed soft/hard substrates, and have an Arctic distribution. These functional traits correspond primarily to taxa such as the crinoid *Bathycrinus* cf. *carpenterii*, the small sea anemone cf. *Bathyphellia margaritacea*, and the sponge morphotype 'small round sponge'. It should be noted, however, that the proportional increase of those functional traits was primarily due to the decrease in density of *E. heckeri* rather than the increase in density of the other mentioned taxa (see Fig. 3).

Strong shifts between suspension feeders and deposit feeders, similar to those observed from 2016 onward in our study, have also been documented at the long-term observatory Station M in the Northeast Pacific Ocean (Kuhnz et al., 2014, 2020). There, these shifts occurred within two years and were linked to significant increases in food supply (Kuhnz et al., 2014, 2020). Differences in the densities of trophic groups are often driven by variations in both quality and quantity of available food (Campanyà-Llovet et al., 2017; McMahon et al., 2006). Specifically, inputs of fresh organic matter tend to increase the density of deposit feeders such as *E. heckeri*, whereas suspension feeders were found to

respond positively to increased lipid concentration, and predators did not show any response to changes in food quality (Campanyà-Llovet et al., 2017; Wieking and Kröncke, 2005). This suggests that changes in food quality reaching the seafloor likely drove the increase in deposit feeders observed in our study. Additionally, most deposit feeders, including *E. heckeri*, are mobile organisms capable of actively seeking and switching foraging areas (Iken et al., 2001). This mobility also allows them to migrate to or from adjacent areas depending on food availability, as observed at the shallower HAUSGARTEN station HG-I (Meyer et al., 2013).

The benthic communities at all stations were characterized by taxa associated with soft substrate, which is to be expected as most HAUSGARTEN stations are characterized primarily by soft sediments (Soltwedel et al., 2005). Hard and biological features, consisting of (drop-)stones, sponge and crinoid stalks, are primarily used by epibiotic suspension feeders due to their advantageous elevated position in the water column (Gutt and Schickan, 1998; Meyer et al., 2016). These substrates increase habitat heterogeneity and therefore epifauna density, influencing the community structure (Meyer et al., 2016; Zhulay et al., 2019). Over the six-year period, however, changes in proportions of substratum affinity were mostly driven by increased proportions of organisms associated with soft substratum, rather than decreased proportions of organisms associated with hard/biological substratum.

Regarding the zoogeography, increased proportions of Arctic-boreal taxa over time were observed, especially at N3 but also at the other stations in certain years. Lowest proportions of Arctic taxa in general were observed at S3, the southern-most station. As the Arctic continues to warm, poleward expansion of boreal taxa and range restriction of Arctic taxa is predicted (Renaud et al., 2015). Arctic fish species in the Barents Sea, characterized by bottom-dwelling benthivores, have been observed to be rapidly replaced by boreal taxa in response to warming (Frainer et al., 2017). Studies from other regions of the Arctic Ocean detected similar trends. In the Beaufort Sea and the Chukchi Borderland, Atlantic-boreal taxa dominate the epibenthic community due to the continuous inflow of warmer water from the Atlantic into the Arctic Ocean, demonstrating the connectivity between Atlantic-Arctic deep--water layers and the Pacific Arctic region (Ravelo et al., 2020; Zhulay et al., 2019). In our study, the dominance of Arctic-boreal taxa in certain years was predominantly due to increased densities of *E. heckeri*. However, at the southern-most station S3, high densities of this Arctic-boreal taxon co-occurred with high densities of taxa of undefined zoogeography, such as the sponge morphotype 'small round sponge', and low densities of Arctic taxa, such as the crinoid *Bathycrinus* cf. *carpenterii*. As a result, the proportion of Arctic taxa remained low in all years. One possible explanation is that S3 is more strongly affected by the inflow of warm Atlantic waters due to its location.

4.2. Influence of environmental variables on megafauna community composition

To identify and explain the temporal patterns for the wider HAUSGARTEN area, the community composition of the benthic megafauna and the corresponding environmental variables were analyzed jointly. Since variations in environmental variables were strongly associated with spatial rather than temporal differences in community composition, spatio-temporal dynamics are discussed separately in Section 4.2.1 (spatial comparison) and Section 4.2.2 (temporal comparison).

4.2.1. Spatial comparison of megafauna communities and environmental characteristics between stations

Spatial differences in megafauna community composition, habitat features, and biogenic sediment compounds were evident among the three HAUSGARTEN stations. These differences could be explained by station-specific environmental conditions, given the distance between stations (>50 km) and their varying proximity to the ice edge. The northern station N3 and the central station HG-IV are located close to the ice edge and are partially covered by sea ice throughout the year, whereas the southern station S3 remains predominantly ice-free (Soltwedel et al., 2016). The vicinity to the ice edge was reported to influence the phytoplankton community composition, resulting in contrasting quality and quantity of phytodetrital flux from the surface ocean to the seafloor (Bauerfeind et al., 2009; Fadeev et al., 2021; von Appen et al., 2021). This may have contributed to the observed variation in biogenic sediment compounds across stations, with the highest organic carbon levels recorded at N3 and the lowest at S3, ultimately also affecting the benthic megafauna communities (Reed et al., 2021; Rybakova et al., 2019). Additionally, the vicinity to the ice edge may have influenced the distribution of habitat features. Stones entrained in glacial ice and transported out to the sea by melting icebergs (Bennett et al., 1996) may be released along the ice edge, potentially explaining the higher (drop-)stone density at N3, the station closest to the ice edge. Dropstones are known to increase habitat heterogeneity and provide hard substrata for sessile organisms (Meyer et al., 2016; Schulz et al., 2010), such as the sponges *Caulophacus arcticus* and *Cladorhiza gelida*. These species were not only observed predominantly at N3, but dead colonies were also represented in the habitat feature 'sponge debris', which largely characterized this station. This suggests that the habitat at N3 was of greater structural complexity, which may explain the higher observed total megafauna densities. In contrast, sponge debris and (drop-)stones had little influence at the southernmost station S3, which was primarily characterized by burrows of the amphipod *Neohela lamia*. These burrows were virtually absent at N3, pointing to an absence of *N. lamia* at that station, although this was not the case in earlier years (Taylor et al., 2017). Unfortunately, little is known about the ecology of *N. lamia*, which limits our ability to fully explain the observed spatial patterns. The habitat at the intermediate station HG-IV appears to form a transition zone between the northern station N3 and the southern station S3. However, the substantial variation in megafauna community composition at HG-IV, as observed on the dbRDA plot, was likely due to unaccounted environmental variables. These spatial variations in habitat features and sediment biogenic compounds appear to be primary drivers of the observed differences in megafauna community composition across stations, independent of temporal variability.

4.2.2. Temporal trends of megafauna communities and environmental characteristics across all stations

Although temporal differences in biogenic sediment compounds could not statistically explain the variability in megafauna community composition in our study, high concentrations of sediment-bound phaeopigments and organic carbon content were observed in the same year that megafaunal densities peaked at N3 and HG-IV. High organic carbon content is an indicator of high food availability, which was found to correlate with increased megafauna abundances (Campanyà-Llovet et al., 2017). High concentrations of phaeopigments combined with low chlorophyll *a* concentrations indicate low quality or more degraded phytodetrital matter on the seafloor (Schewe and Soltwedel, 2003), possibly due to variations in the composition of the phytoplankton community (FitzGeorge-Balfour et al., 2010; McMahon et al., 2006) or due to different rates of degradation in the water column (Fadeev et al., 2021). Thus, we suggest that the high levels of low-quality phytodetrital matter in 2019 may have been beneficial, particularly for the opportunistic sea cucumber *E. heckeri,* as we observed a strong increase in density in the same year. For the southern station, S3, the highest phaeopigment content was found in 2021, and the highest organic carbon content in 2016, while megafaunal density peaked in 2017. Interestingly, bacterial activity also peaked in 2017 at S3. This may indicate that higher phytodetrital input earlier in 2017 facilitated higher bacterial activity and caused a higher megafaunal density at the time of sampling. High microbial activity has been reported to be particularly beneficial to deposit-feeding organisms, as more organic material becomes available after microbial degradation (Lovvorn et al., 2005). In fact, deposit-feeding organisms represented the highest proportion of

the total megafauna community at station S3 in 2017.

Temporal trends in environmental variables affecting the benthic megafauna are more difficult to identify than spatial differences. One reason could be a mismatch in certain years between the timing of the survey and the deposition of organic material at the seafloor after the algal bloom. Photographic surveys took place over a few hours each year at some time between June and September. Phytoplankton blooms, and subsequent phytodetrital flux, occur seasonally in the Arctic Ocean in a bimodal pattern in May/June and August/September (Bauerfeind et al., 2009), however, the intensity and timing of the export flux is largely dependent on oceanographic conditions in the surface ocean (von Appen et al., 2021) and thus on the composition of the phytoplankton community (Dybwad et al., 2021). The exact timing of the export flux reaching the seafloor is therefore poorly constrained on an annual basis. Image data collected before the post-bloom period might not capture the full extent of recruitment and/or migration of megafauna into an area with elevated phytodetrital flux, especially given that the response of communities to increased phytodetritus at the seafloor can take 0.5-1 years (Billett et al., 2010; Soto et al., 2010) or varies by species and life stage of particular organisms or cohorts. The temporal relation and time lag between the event and the photographic surveys remain uncertain. Complex environmental interactions increase the difficulty of disentangling parameters responsible for variations in benthic megafauna community composition. Environmental parameters can act additively or synergistically, thereby increasing the effect of other parameters (Crain et al., 2008). Additionally, given the relatively short time-series analysis of six years, our observations might be part of natural variability in megafaunal community composition, rather than climate-induced changes, which may only be detectable after ~32 years of observation (Henson et al., 2016).

4.3. Long-term variability in benthic megafauna densities

One of the most striking findings of our study is the pronounced decline in densities of four representative benthic megafauna taxa – *Gersemia fruticosa* (soft coral), *Bathycrinus* cf. *carpenterii* (crinoid), *Kolga hyalina* (sea cucumber), and the 'purple anemone' morphotype – when comparing the earlier period (2002/2004–2015) with recent data (2016–2021). This decline was consistent across all three HAUSGARTEN stations, with reductions ranging from 28% (for *B.* cf. *carpenterii* at N3) to as high as 93% (for *G. fruticosa* at HG-IV). These results suggest substantial long-term changes in benthic megafauna communities, which parallel reported declines in smaller benthic fauna such as macro- and meiofauna at HAUSGARTEN (Schnier et al., 2025; Soltwedel et al., 2020; Vedenin et al., 2019). However, unlike megafauna, macrofaunal declines were mainly restricted to Crustacea (Vedenin et al., 2019), while meiofaunal decreases were most pronounced at shallower sites and attributed to reductions in nutritional food supply (Schnier et al., 2025; Soltwedel et al., 2020). The observed decline in megafauna densities may be linked to shifts in food quality and availability. Although primary productivity in the upper Arctic Ocean has generally increased over the last two decades, changes in phytoplankton community composition (Ardyna and Arrigo, 2020) could lead to the deposition of less nutritious phytodetrital matter on the seafloor in the long term, negatively affecting benthic consumers. This is supported by the strong link between benthic density patterns and biogeochemical sediment proxies such as chlorophyll *a* and organic carbon in our study.

Importantly, taxon-specific responses were evident. While all four focal taxa declined over time, *E. heckeri*, a smaller sea cucumber and deposit feeder, showed notable density increases in some recent years, indicating differing ecological strategies and environmental sensitivities even among taxa with similar trophic roles (Durden et al., 2020). Unfortunately, *E. heckeri* could not be included in the long-term comparison due to its small size and uncertain detectability in earlier, lower-resolution imagery. This highlights a methodological constraint in benthic long-term studies relying on photographic data. Other limitations include differences in seafloor area surveyed and density calculation methods between the two periods. However, given the consistent declining trends observed across multiple taxa and stations, we consider the results robust rather than artifacts of methodological variation. To improve future long-term assessments, increasing image resolution to include smaller fauna like *E. heckeri* would be beneficial, although this comes at the cost of losing some historical data continuity. Overall, these findings underscore the complexity of benthic community dynamics in the Arctic and emphasize the need to consider taxon-specific traits, environmental drivers, and methodological consistency in long-term ecological monitoring.

5. Conclusion

Our results demonstrate temporal short-term variation in the taxonomic and functional composition of the benthic megafauna community at the HAUSGARTEN observatory over the six-year study period, primarily driven by changes in the density of the small opportunistic sea cucumber *Elpidia heckeri*. Although elevated phaeopigments and organic carbon content were observed in the same year, megafauna density peaked for N3 and HG-IV; a general trend in benthic megafauna community composition and environmental parameters for the wider HAUSGARTEN area was not observed. The joint analysis showed that the environmental parameters explained spatial (across stations) rather than temporal (across years) differences of the megafauna community composition. The environmental conditions prevailing at each station were different, and thus, the complex responses of the megafauna communities to changing environmental conditions over time. Long-term trends for selected taxa revealed a declining trend over time, potentially due to a decreasing quality of phytodetrital matter at the seafloor. However, predictions about trends for the entire megafauna community cannot be made due to a lack of observation for smaller organisms.

This study highlights the highly dynamic nature of Arctic benthic megafauna communities and their complex responses to local environmental change. The pronounced variability and substantial declines in population densities, compared to earlier observations, emphasize the urgent need to extend time-series studies both temporally and spatially, for example, by increasing spatial coverage or by including intra-annual observations to infer seasonal variation patterns, in order to make robust projections about the future state of Arctic deep-sea ecosystems.

CRediT authorship contribution statement

Lilian Boehringer: Writing – review & editing, Writing – original draft, Visualization, Validation, Methodology, Investigation, Formal analysis, Data curation. **Melanie Bergmann:** Writing – review & editing, Resources, Conceptualization. **Christiane Hasemann:** Writing – review & editing, Investigation, Formal analysis. **James Taylor:** Writing – review & editing, Validation. **Jennifer Dannheim:** Writing – review & editing, Writing – original draft, Methodology.

Funding sources

Ship time on RV Polarstern was provided under grants AWI_PS99_00, AWI_PS107_12, AWI_PS114_01, AWI_PS121_01, AWI_PS126_01. LB was funded by the program INSPIRES III of the Alfred Wegener Institute.

Declaration of competing interest

The authors declare that they have no known competing financial interests or personal relationships that could have appeared to influence the work reported in this paper.

Acknowledgements

We would like to thank the officers and the crew of RV Polarstern during the expeditions PS99, PS107, PS114, PS121, and PS126, and of RV Maria S. Merian during the expeditions MSM77 and MSM95 for their support and experience. We would also like to thank the cruise leaders and all scientists and the technical support staff who were involved in conducting the camera surveys, multiple corer deployments, gear maintenance, and sediment analyses. We are especially grateful to U. Hoge for technically supporting the OFOS/OFOBS and A. Pappert and numerous volunteers and students for assisting in sediment analyses. We would also like to thank three anonymous reviewers for their valuable input on the manuscript. Finally, we acknowledge the support of the Open Access Publication Funds of Alfred Wegener Institute Helmholtz Centre for Polar and Marine Research.

Appendix A. Supplementary data

Supplementary data to this article can be found online at https://doi.org/10.1016/j.dsr2.2026.105621.

Data availability

Megafauna densities, functional traits, and habitat features per image are available from Mendeley data under the following https://doi.org/10.17632/8p8w4jb3ff.1. Seafloor images are permanently stored with the long-term repository PANGAEA (Felden et al., 2023) for PS99 (Bergmann and Schewe, 2017a, 2017b, 2017c), PS107 (Bergmann, 2018a, 2018b, 2018c), PS114 (Bergmann, 2018d), MSM77 (Boehringer and Bergmann, 2026), PS121 (Purser, 2021a, 2021b, 2021c), MSM95 (Purser et al., 2021), PS126 (Boehringer et al., 2026).

References

Anderson, M.J., Gorley, R.N., Clarke, K.R., 2008. PERMANOVA+ for PRIMER: Guide to Software and Statistical Methods. Primer-E Plymouth, UK.

Ardyna, M., Arrigo, K.R., 2020. Phytoplankton dynamics in a changing Arctic Ocean. Nat. Clim. Change 10, 892–903. https://doi.org/10.1038/s41558-020-0905-y.

Assmy, P., Fernández-Méndez, M., Duarte, P., Meyer, A., Randelhoff, A., Mundy, C.J., Olsen, L.M., Kauko, H.M., Bailey, A., Chierici, M., Cohen, L., Doulgeris, A.P., Ehn, J. K., Fransson, A., Gerland, S., Hop, H., Hudson, S.R., Hughes, N., Itkin, P., Johnsen, G., King, J.A., Koch, B.P., Koenig, Z., Kwasniewski, S., Laney, S.R., Nicolaus, M., Pavlov, A.K., Polashenski, C.M., Provost, C., Rösel, A., Sandbu, M., Spreen, G., Smedsrud, L.H., Sundfjord, A., Taskjelle, T., Tatarek, A., Wiktor, J., Wagner, P.M., Wold, A., Steen, H., Granskog, M.A., 2017. Leads in arctic pack ice enable early phytoplankton blooms below snow-covered sea ice. Sci. Rep. 7, 1–9. https://doi.org/10.1038/srep40850.

Bauerfeind, E., Nöthig, E.-M., Beszczynska, A., Fahl, K., Kaleschke, L., Kreker, K., Klages, M., Soltwedel, T., Lorenzen, C., Wegner, J., 2009. Particle sedimentation patterns in the eastern fram strait during 2000-2005: results from the arctic long-term observatory HAUSGARTEN. Deep-Sea Res. Part A Oceanogr. Res. Pap. 56, 1471–1487. https://doi.org/10.1016/j.dsr.2009.04.011.

Bennett, M.R., Doyle, P., Mather, A.E., 1996. Dropstones: their origin and significance. Palaeogeogr. Palaeoclimatol. Palaeoecol. 121, 331–339.

Bergmann, M., 2018a. Seabed photographs taken along OFOS profile PS107_36-6 during POLARSTERN cruise PS107. https://doi.org/10.1594/PANGAEA.896656.

Bergmann, M., 2018b. Seabed photographs taken along OFOS profile PS107_6-12 during POLARSTERN cruise PS107. https://doi.org/10.1594/PANGAEA.896654.

Bergmann, M., 2018c. Seabed photographs taken along OFOS profile PS107_2-20 during POLARSTERN cruise PS107. https://doi.org/10.1594/PANGAEA.896653.

Bergmann, M., 2018d. Seabed photographs taken along OFOS profile PS114_33-3 during POLARSTERN cruise PS114. https://doi.org/10.1594/PANGAEA.895102.

Bergmann, M., Dannheim, J., Bauerfeind, E., Klages, M., 2009. Trophic relationships along a bathymetric gradient at the deep-sea observatory HAUSGARTEN. Deep-Sea Res. Part A Oceanogr. Res. Pap. 56, 408–424. https://doi.org/10.1016/j.dsr.2008.10.004.

Bergmann, M., Schewe, I., 2017a. In: Seabed Photographs Taken Along OFOS Profile PS99/056-1 During POLARSTERN Cruise PS99, 2. https://doi.org/10.1594/PANGAEA.874002.

Bergmann, M., Schewe, I., 2017b. In: Seabed Photographs Taken Along OFOS Profile PS99/042-10 During POLARSTERN Cruise PS99, 2. https://doi.org/10.1594/PANGAEA.874000.

Bergmann, M., Schewe, I., 2017c. In: Seabed Photographs Taken Along OFOS Profile PS99/041-11 During POLARSTERN Cruise PS99, 2. https://doi.org/10.1594/PANGAEA.873999.

Bergmann, M., Soltwedel, T., Klages, M., 2011. The interannual variability of megafaunal assemblages in the arctic deep sea: preliminary results from the HAUSGARTEN observatory (79°N). Deep-Sea Res. Part A Oceanogr. Res. Pap. 58, 711–723. https://doi.org/10.1016/j.dsr.2011.03.007.

Beszczynska-Möller, A., Fahrbach, E., Schauer, U., Hansen, E., 2012. Variability in Atlantic water temperature and transport at the entrance to the Arctic Ocean, 1997-2010. ICES J. Mar. Sci. 69, 852–863. https://doi.org/10.1093/icesjms/fss056.

Bett, B.J., Malzone, M.G., Narayanaswamy, B.E., Wigham, B.D., 2001. Temporal variability in phytodetritus and megabenthic activity at the seabed in the deep northeast Atlantic. Prog. Oceanogr. 50, 349–368. https://doi.org/10.1016/S0079-6611(01)00066-0.

Billett, D.S.M., Bett, B.J., Reid, W.D.K., Boorman, B., Priede, I.G., 2010. Long-term change in the abyssal NE Atlantic: the "Amperima Event" revisited. Deep-Sea Res. Part II 57, 1406–1417. https://doi.org/10.1016/j.dsr2.2009.02.001.

Bluhm, B.A., Ambrose Jr., W.G., Bergmann, M., Clough, L.M., Gebruk, A.V., Hasemann, C., Iken, K., Klages, M., Macdonald, I.R., Renaud, P.E., Schewe, I., Soltwedel, T., Wlodarska-Kowalczuk, M., 2011. Diversity of the arctic deep-sea benthos. Mar. Biodivers. 41, 87–107. https://doi.org/10.1007/s12526-010-0078-4.

Bluhm, B.A., Kosobokova, K.N., Carmack, E.C., 2015. A tale of two basins: an integrated physical and biological perspective of the deep Arctic Ocean. Prog. Oceanogr. 139, 89–121. https://doi.org/10.1016/j.pocean.2015.07.011.

Boehringer, L., Bergmann, M., 2026. Ocean floor observation system (OFOS) seafloor images of the fram strait collected during RV MARIA S. MERIAN cruise MSM77. https://doi.org/10.1594/PANGAEA.989682.

Boehringer, L., Bergmann, M., Purser, A., 2026. Ocean floor. In: Observation and Bathymetry System (OFOBS) Seafloor Images of the Fram Strait Collected During RV POLARSTERN Cruise PS126. https://doi.org/10.1594/PANGAEA.989651.

Buhl-Mortensen, L., Vanreusel, A., Gooday, A.J., Levin, L.A., Priede, I.G., Buhl-Mortensen, P., Gheerardyn, H., King, N.J., Raes, M., 2010. Biological structures as a source of habitat heterogeneity and biodiversity on the deep ocean margins. Mar. Ecologist 31, 21–50. https://doi.org/10.1111/j.1439-0485.2010.00359.x.

Campanyà-Llovet, N., Snelgrove, P.V.R., Parrish, C.C., 2017. Rethinking the importance of food quality in marine benthic food webs. Prog. Oceanogr. 156, 240–251. https://doi.org/10.1016/j.pocean.2017.07.006.

Clarke, K.R., 1993. Non-parametric multivariate analyses of changes in community structure. Aust. J. Ecol. 18, 117–143. https://doi.org/10.1111/j.1442-9993.1993.tb00438.x.

Clarke, K.R., Warwick, R.M., 2001. Change in Marine Communities: an Approach to Statistical Analysis and Interpretation, second ed. PRIMER-E, Plymouth.

Crain, C.M., Kroeker, K., Halpern, B.S., 2008. Interactive and cumulative effects of multiple human stressors in marine systems. Ecol. Lett. 11, 1304–1315.

de Steur, L., Hansen, E., Gerdes, R., Karcher, M., Fahrbach, E., Holfort, J., 2009. Freshwater fluxes in the east Greenland current: a decade of observations. Geophys. Res. Lett. 36, L23611. https://doi.org/10.1029/2009GL041278.

Degen, R., Faulwetter, S., 2019. The arctic traits database – a repository of arctic benthic invertebrate traits. Earth Syst. Sci. Data 11, 301–322. https://doi.org/10.5194/essd-11-301-2019.

Durden, J.M., Bett, B.J., Huffard, C.L., Pebody, C., Ruhl, H.A., Smith, K.L., 2020. Response of deep-sea deposit-feeders to detrital inputs: a comparison of two abyssal time-series sites. Deep-Sea Res. Part II Top. Stud. Oceanogr. 173. https://doi.org/10.1016/j.dsr2.2019.104677.

Durden, J.M., Bett, B.J., Schoening, T., Morris, K.J., Nattkemper, T., Ruhl, H.A., 2016a. Comparison of image annotation data generated by multiple investigators for benthic ecology. Mar. Ecol. Prog. Ser. 552, 61–70. https://doi.org/10.3354/meps11775.

Durden, J.M., Schoening, T., Althaus, F., Friedman, A., Garcia, R., Glover, A.G., Greinert, J., Jacobsen Stout, N., Jones, D.O.B., Jordt, A., Kaeli, J.W., Koser, K., Kuhnz, L.A., Lindsay, D., Morris, K.J., Nattkemper, T.W., Osterloff, J., Ruhl, H.A., Singh, H., Tran, M., Bett, B.J., 2016b. Perspectives in visual imaging for marine biology and ecology: from acquisition to understanding. Oceanogr. Mar. Biol. Annu. Rev. 54, 1–72.

Dybwad, C., Assmy, P., Olsen, L.M., Peeken, I., Nikolopoulos, A., Krumpen, T., Randelhoff, A., Tatarek, A., Wiktor, J.M., Reigstad, M., 2021. Carbon export in the seasonal sea ice zone north of Svalbard from winter to late summer. Front. Mar. Sci. 7, 1–21. https://doi.org/10.3389/fmars.2020.525800.

Fadeev, E., Rogge, A., Ramondenc, S., Nöthig, E.-M., Wekerle, C., Bienhold, C., Salter, I., Waite, A.M., Hehemann, L., Boetius, A., Iversen, M.H., 2021. Sea ice presence is linked to higher carbon export and vertical microbial connectivity in the eurasian Arctic Ocean. Commun. Biol. 4, 1–13. https://doi.org/10.1038/s42003-021-02776-w.

Felden, J., Möller, L., Schindler, U., Huber, R., Schumacher, S., Koppe, R., Diepenbroek, M., Glöckner, F.O., 2023. PANGAEA - Data publisher for Earth & environmental science. Sci. Data 10, 347. https://doi.org/10.1038/s41597-023-02269-x.

FitzGeorge-Balfour, T., Billett, D.S.M., Wolff, G.A., Thompson, A., Tyler, P.A., 2010. Phytopigments as biomarkers of selectivity in abyssal holothurians; interspecific differences in response to a changing food supply. Deep-Sea Res. Part II Top. Stud. Oceanogr. 57, 1418–1428. https://doi.org/10.1016/j.dsr2.2010.01.013.

Frainer, A., Primicerio, R., Kortsch, S., Aune, M., Dolgov, A.V., Fossheim, M., Aschan, M. M., 2017. Climate-driven changes in functional biogeography of arctic marine fish communities. Proc. Natl. Acad. Sci. U. S. A 114, 12202–12207. https://doi.org/10.1073/pnas.1706080114.

Górska, B., Gromisz, S., Legeżyńska, J., Soltwedel, T., Włodarska-Kowalczuk, M., 2022. Macrobenthic diversity response to the atlantification of the Arctic Ocean (Fram Strait, 79°N) – a taxonomic and functional trait approach. Ecol. Indic. 144. https://doi.org/10.1016/j.ecolind.2022.109464.

Gosselin, M., Levasseur, M., Wheeler, P.A., 1997. New measurements of phytoplankton and ice algal production in the Arctic Ocean. Deep Sea Res. Part II 44, 1623–1644.
Gradinger, R.R., 2009. Sea-ice algae: major contributors to primary production and algal biomass in the Chukchi and beaufort seas during May/June 2002. Deep-Sea Res. Part II Top. Stud. Oceanogr. 56, 1201–1212. https://doi.org/10.1016/j.dsr2.2008.10.016.
Gutt, J., Schickan, T., 1998. Epibiotic relationships in the antarctic benthos. Antarct. Sci. 10, 398–405. https://doi.org/10.1017/s0954102098000480.
Henson, S.A., Beaulieu, C., Ilyina, T., John, J.G., Long, M., Séférian, R., Tjiputra, J., Sarmiento, J.L., 2017. Rapid emergence of climate change in environmental drivers of marine ecosystems. Nat. Commun. 8, 14682.
Henson, S.A., Beaulieu, C., Lampitt, R., 2016. Observing climate change trends in ocean biogeochemistry: when and where. Glob. Change Biol. 22, 1561–1571. https://doi.org/10.1111/gcb.13152.
Hoste, E., Vanhove, S., Schewe, I., Soltwedel, T., Vanreusel, A., 2007. Spatial and temporal variations in deep-sea meiofauna assemblages in the marginal ice zone of the Arctic Ocean. Deep-Sea Res. I 54, 109–129.
Iken, K., Brey, T., Wand, U., Voigt, J., Junghans, P., 2001. Food web structure of the benthic community at the porcupine abyssal plain (NE Atlantic): a stable isotope analysis. Prog. Oceanogr. 50, 383–405. https://doi.org/10.1016/S0079-6611(01)00062-3.
Itkin, M., König, M., Spreen, G., Vongraven, D., Norwegian Polar Institute, 2014. Arctic sea ice frequency with maximum and minimum extents. https://doi.org/10.21334/NPOLAR.2014.A89B2682.
Jakobsson, M., Mayer, L.A., Bringensparr, C., Castro, C.F., Mohammad, R., Johnson, P., Ketter, T., Accettella, D., Amblas, D., An, L., Arndt, J.E., Canals, M., Casamor, J.L., Chauché, N., Coakley, B., Danielson, S., Demarte, M., Dickson, M.-L., Dorschel, B., Dowdeswell, J.A., Dreutter, S., Fremand, A.C., Gallant, D., Hall, J.K., Hehemann, L., Hodnesdal, H., Hong, J., Ivaldi, R., Kane, E., Klaucke, I., Krawczyk, D.W., Kristoffersen, Y., Kuipers, B.R., Millan, R., Masetti, G., Morlighem, M., Noormets, R., Prescott, M.M., Rebesco, M., Rignot, E., Semiletov, I., Tate, A.J., Travaglini, P., Velicogna, I., Weatherall, P., Weinrebe, W., Willis, J.K., Wood, M., Zarayskaya, Y., Zhang, T., Zimmermann, M., Zinglersen, K.B., 2020. The international bathymetric chart of the Arctic Ocean version 4.0. Sci. Data 7, 176. https://doi.org/10.1038/s41597-020-0520-9.
Jones, C.G., Lawton, J.H., Shachak, M., 1994. Organisms as ecosystem engineers. Oikos 69, 373–386. https://doi.org/10.1078/1434-8411-00046.
Kassambara, A., 2023a. Rstatix: Pipe-Friendly Framework for Basic Statistical Tests.
Kassambara, A., 2023b. Ggpubr: "Ggplot2" Based Publication Ready Plots.
Klages, M., Boetius, A., Christensen, J.P., Deubel, H., Piepenburg, D., Schewe, I., Soltwedel, T., 2004. The benthos of arctic seas and its role for the organic carbon cycle at the seafloor. In: Stein, R., MacDonald, R.W. (Eds.), The Organic Carbon Cycle in the Arctic Ocean. Springer Berlin Heidelberg, pp. 139–167. https://doi.org/10.1007/978-3-642-18912-8_6.
Knust, R., 2017. Polar research and supply vessel POLARSTERN operated by the alfred-wegener-institute. J. Large-Scale Res. Facil. JLSRF 3, A119. https://doi.org/10.17815/jlsrf-3-163.
Kremenetskaia, A., Ezhova, O., Drozdov, A.L., Rybakova, E., Gebruk, A., 2020. On the reproduction of two deep-sea arctic holothurians, Elpidia heckeri and Kolga hyalina (Holothuroidea:Elpidiidae). Invertebr. Reprod. Dev. 64, 33–47. https://doi.org/10.1080/07924259.2019.1692915.
Kuhnz, L.A., Ruhl, H.A., Huffard, C.L., Smith, K.L., 2020. Benthic megafauna assemblage change over three decades in the abyss: variations from species to functional groups. Deep-Sea Res. Part II Top. Stud. Oceanogr. 173. https://doi.org/10.1016/j.dsr2.2020.104761.
Kuhnz, L.A., Ruhl, H.A., Huffard, C.L., Smith, K.L., 2014. Rapid changes and long-term cycles in the benthic megafaunal community observed over 24 years in the abyssal northeast Pacific. Prog. Oceanogr. 124, 1–11. https://doi.org/10.1016/j.pocean.2014.04.007.
Laliberte, E., Legendre, P., Shipley, B., 2014. FD: Measuring Functional Diversity from Multiple Traits, and Other Tools for Functional Ecology.
Langenkämper, D., Zurowietz, M., Schoening, T., Nattkemper, T.W., 2017. Biigle 2.0 - browsing and annotating large marine image collections. Front. Mar. Sci. 4. https://doi.org/10.3389/fmars.2017.00083.
Legendre, P., Anderson, M.J., 1999. Distance-based redundancy analysis: testing multispecies responses in multifactorial ecological experiments. Ecol. Monogr. 69, 1–24. https://doi.org/10.2307/2657192.
Lovvorn, J.R., Cooper, L.W., Brooks, M.L., De Ruyck, C.C., Bump, J.K., Grebmeier, J.M., 2005. Organic matter pathways to zooplankton and benthos under pack ice in late winter and open water in late summer in the north-central Bering Sea. Mar. Ecol. Prog. Ser. 291.
MacDonald, I.R., Bluhm, B.A., Iken, K., Gagaev, S., Strong, S., 2010. Benthic macrofauna and megafauna assemblages in the arctic deep-sea Canada basin. deep-sea res. Part II top. Stud. Oceanogr. 57, 136–152. https://doi.org/10.1016/j.dsr2.2009.08.012.
Mayot, N., Matrai, P.A., Arjona, A., Bélanger, S., Marchese, C., Jaegler, T., Ardyna, M., Steele, M., 2020. Springtime export of arctic sea ice influences phytoplankton production in the Greenland Sea. J. Geophys. Res., Oceans 125, 1–16. https://doi.org/10.1029/2019JC015799.
McArdle, B.H., Anderson, M.J., 2001. Fitting multivariate models to community data: a comment on distance-based redundancy analysis. Ecology 82, 290–297. https://doi.org/10.2307/2680104.
McMahon, K.W., Ambrose Jr., W.G., Johnson, B.J., Sun, M.Y., Lopez, G.R., Clough, L.M., Carroll, M.L., 2006. Benthic community response to ice algae and phytoplankton in Ny Ålesund, Svalbard. Mar. Ecol. Prog. Ser. 310, 1–14. https://doi.org/10.3354/meps310001.
Metfies, K., 2020. In: The Expedition PS121 of the Research Vessel POLARSTERN to the Fram Strait in 2019, Berichte Zur Polar- Und Meeresforschung = Reports on Polar and Marine Research. https://doi.org/10.2312/BzPM_0738_2020. Bremerhaven, Germany.
Meyer, K.S., Bergmann, M., Soltwedel, T., 2013. Interannual variation in the epibenthic megafauna at the shallowest station of the HAUSGARTEN observatory (79 N, 6 E). Biogeosciences 10, 3479–3492. https://doi.org/10.5194/bg-10-3479-2013.
Meyer, K.S., Young, C.M., Sweetman, A.K., Taylor, J., Soltwedel, T., Bergmann, M., 2016. Rocky islands in a sea of mud: biotic and abiotic factors structuring deep-sea dropstone communities. Mar. Ecol. Prog. Ser. 556, 45–57. https://doi.org/10.3354/meps11822.
Meyer-Kaiser, K.S., Nuñez, K., Soltwedel, T., Bergmann, M., 2025. Long-term changes in deep-sea megafauna community structure in the eastern Fram strait (Arctic Ocean). Mar. Ecol. Prog. Ser. 770, 1–14. https://doi.org/10.3354/meps14933.
Mintenbeck, K., Jacob, U., Knust, R., Arntz, W.E., Brey, T., 2007. Depth-dependence in stable isotope ratio δ15N of benthic POM consumers: the role of particle dynamics and organism trophic guild. Deep-Sea Res. Part A Oceanogr. Res. Pap. 54, 1015–1023. https://doi.org/10.1016/j.dsr.2007.03.005.
Oksanen, J., Simpson, G., Blanchet, F., Kindt, R., Legendre, P., Minchin, P., O'Hara, R., Solymos, P., Stevens, M., Szoecs, E., Wagner, H., Barbour, M., Bedward, M., Bolker, B., Borcard, D., Carvalho, G., Chirico, M., De Caceres, M., Durand, S., Evangelista, H., FitzJohn, R., Friendly, M., Furneaux, B., Hannigan, G., Hill, M., Lahti, L., McGlinn, D., Ouellette, M., Ribeiro Cunha, E., Smith, T., Stier, A., Ter Braak, C., Weedon, J., 2022. Vegan: Community Ecology Package.
Pedersen, T.L., 2025. Patchwork: the Composer of Plots.
Pielou, E.C., 1966. The measurement of diversity in different types of biological collections. J. Theor. Biol. 13, 131–144.
Piepenburg, D., Blackburn, T.H., von Dorrien, C.F., Gutt, J., Hall, P.O., Hulth, S., Kendall, M.A., Opalinski, K.W., Rachor, E., Schmid, M.K., 1995. Partitioning of benthic community respiration in the Arctic (northwestern Barents Sea). Mar. Ecol. Prog. Ser. 118, 199–214. https://doi.org/10.3354/meps118199.
Piepenburg, D., von Dorrien, C.F., Schmid, M.K., Chernova, N.V., Neyelov, A.V., Gutt, J., Rachor, E., Saldanha, L., 1996. Megabenthic communities in the waters around Svalbard. Polar Biol. 16, 431–446. https://doi.org/10.1007/bf02390425.
Purser, A., 2021a. Seabed photographs taken along OFOS profile PS121_49-1 during POLARSTERN cruise PS121. https://doi.org/10.1594/PANGAEA.929979.
Purser, A., 2021b. Seabed photographs taken along OFOS profile PS121_7-4 during POLARSTERN cruise PS121. https://doi.org/10.1594/PANGAEA.929976.
Purser, A., 2021c. Seabed photographs taken along OFOS profile PS121_10-10 during POLARSTERN cruise PS121. https://doi.org/10.1594/PANGAEA.929977.
Purser, A., Boehringer, L., Hehemann, L., Hoge, U., Merten, V., Dreutter, S., 2021. OFOBS seafloor images from the Svalbard archipelago and fram strait, collected during RV MARIA S. MERIAN expedition MSM95. https://doi.org/10.1594/PANGAEA.928815.
Purser, A., Hoge, U., Busack, M., Hagemann, J., Dauer, E., Korfman, N., Boehringer, L., Merten, V., Priest, T., Dreutter, S., Warnke, F., Hehemann, L., 2020. Arctic seafloor integrity cruise no. MSM95 (GPF 19-2_05). Maria Merian Berichte.
Purser, A., Marcon, Y., Dreutter, S., Hoge, U., Sablotny, B., Hehemann, L., Lemburg, J., Dorschel, B., Biebow, H., Boetius, A., 2019. Ocean floor observation and bathymetry system (OFOBS): a new towed camera/sonar system for deep-sea habitat surveys. IEEE J. Ocean. Eng. 44, 87–99. https://doi.org/10.1109/JOE.2018.2794095.
Quéric, N.V., Soltwedel, T., 2007. Impact of small-scale biogenic sediment structures on bacterial distribution and activity in arctic deep-sea sediments. Mar. Ecol. 28, 66–74.
R Core Team, 2024. R: a Language and Environment for Statistical Computing.
Rantanen, M., Karpechko, A.Yu, Lipponen, A., Nordling, K., Hyvärinen, O., Ruosteenoja, K., Vihma, T., Laaksonen, A., 2022. The arctic has warmed nearly four times faster than the globe since 1979. Commun. Earth Environ. 3, 168. https://doi.org/10.1038/s43247-022-00498-3.
Ravelo, A.M., Bluhm, B.A., Foster, N., Iken, K., 2020. Biogeography of epibenthic assemblages in the central beaufort sea. Mar. Biodivers. 50. https://doi.org/10.1007/s12526-019-01036-9.
Reed, A.J., Godbold, J.A., Solan, M., Grange, L.J., 2021. Reproductive traits and population dynamics of benthic invertebrates indicate episodic recruitment patterns across an arctic polar. Front. Ecol. Evol. 11, 6900–6912. https://doi.org/10.1002/ece3.7539.
Renaud, P.E., Sejr, M.K., Bluhm, B.A., Sirenko, B., Ellingsen, I.H., 2015. The future of arctic benthos: expansion, invasion, and biodiversity. Prog. Oceanogr. 139, 244–257. https://doi.org/10.1016/j.pocean.2015.07.007.
Ruhl, H.A., 2007. Abundance and size distribution dynamics of abyssal epibenthic megafauna in the northeast Pacific. Ecology 88, 1250–1262. https://doi.org/10.1890/06-0890.
Rybakova, E., Kremenetskaia, A., Vedenin, A., Boetius, A., Gebruk, A.V., 2019. Deep-sea megabenthos communities of the eurasian central arctic are influenced by ice-cover and sea-ice algal falls. PLoS One 14, 1–27. https://doi.org/10.1371/journal.pone.0211009.
Schewe, I., 2018. In: The Expedition PS107 of the Research Vessel POLARSTERN to the Fram Strait and the AWI-HAUSGARTEN in 2017, Berichte Zur Polar- Und Meeresforschung = Reports on Polar and Marine Research. https://doi.org/10.2312/BzPM_0717_2018. Bremerhaven, Germany.
Schewe, I., Soltwedel, T., 2003. Benthic response to ice-edge-induced particle flux in the Arctic Ocean. Polar Biol. 26, 610–620. https://doi.org/10.1007/s00300-003-0526-8.
Schnier, J., Hasemann, C., Mokievsky, V., Martínez Arbizu, P., Soltwedel, T., 2023. Nematode communities along a bathymetric transect in the deep eastern fram strait (Arctic ocean): interrelations between diversity, function and environment. Front. Mar. Sci. 10. https://doi.org/10.3389/fmars.2023.1271447.

Schnier, J., Soltwedel, T., Grzelak, K., Górska, B., Dannheim, J., Mokievsky, V., Martínez Arbizu, P., Hasemann, C., 2025. Deep-sea nematode community changes over two decades at HAUSGARTEN observatory (Fram strait, Arctic Ocean). Mar. Ecol. Prog. Ser. 770, 25–43. https://doi.org/10.3354/meps14948.

Schoening, T., Purser, A., Langenkämper, D., Suck, I., Taylor, J., Cuvelier, D., Lins, L., Simon-Lledó, E., Marcon, Y., Jones, D.O.B., Nattkemper, T., Köser, K., Zurowietz, M., Greinert, J., Gomes-Pereira, J., 2020. Megafauna community assessment of polymetallic-nodule fields with cameras: platform and methodology comparison. Biogeosciences 17, 3115–3133. https://doi.org/10.5194/bg-17-3115-2020.

Schulz, M., Bergmann, M., von Juterzenka, K., Soltwedel, T., 2010. Colonisation of hard substrata along a channel system in the deep Greenland Sea. Polar Biol. 33, 1359–1369. https://doi.org/10.1007/s00300-010-0825-9.

Shannon, C.E., Weaver, W., 1963. In: The Mathematical Theory of Communication, 131. Univ. Ill. Press, Urbana.

Smith, K.L., Ruhl, H.A., Bett, B.J., Billett, D.S.M., Lampitt, R.S., Kaufmann, R.S., 2009. Climate, carbon cycling, and deep-ocean ecosystems. Proc. Natl. Acad. Sci. U. S. A 106, 19211–19218. https://doi.org/10.1073/pnas.0908322106.

Soltwedel, T., 2021. In: The Expedition PS126 of the Research Vessel POLARSTERN to the Fram Strait in 2021, Berichte Zur Polar- Und Meeresforschung = Reports on Polar and Marine Research. https://doi.org/10.48433/BzPM_0757_2021. Bremerhaven, Germany.

Soltwedel, T., 2016. In: The Expeditions PS99.1 and PS99.2 of the Research Vessel POLARSTERN to the Fram Strait in 2016, Berichte Zur Polar- Und Meeresforschung = Reports on Polar and Marine Research. https://doi.org/10.2312/BzPM_0704_2016. Bremerhaven, Germany.

Soltwedel, T., Bäger, J., Barz, J., Bergmann, M., Busack, M., Chikina, M., Hagemann, J., Hasemann, C., Hofbauer, M., Hoge, U., Iversen, M., Käß, M.A., Klüver, T., Konrad, C., Lehmenhecker, S., Nordhausen, A., Schewe, I., Sonnek, A., Tekman, M.B., von Jackowski, A., Wenzhoefer, F., Wulff, T., 2019a. Lter HAUSGARTEN 2018 - long-term ecological research in the fram strait, Cruise no. MSM77, September 15 - october 13, 2018. Longyearbyen (Svalbard) - Edinburgh (Scotland). https://doi.org/10.2312/cr_msm77 [WWW Document]. MARIA MERIAN-Berichte.

Soltwedel, T., Bauerfeind, E., Bergmann, M., Bracher, A., Budaeva, N., Busch, K., Cherkasheva, A., Fahl, K., Grzelak, K., Hasemann, C., Jacob, M., Kraft, A., Lalande, C., Metfies, K., Nöthig, E.M., Meyer, K., Quéric, N.V., Schewe, I., Włodarska-Kowalczuk, M., Klages, M., 2016. Natural variability or anthropogenically-induced variation? Insights from 15 years of multidisciplinary observations at the arctic marine LTER site HAUSGARTEN. Ecol. Indic. 65, 89–102. https://doi.org/10.1016/j.ecolind.2015.10.001.

Soltwedel, T., Bauerfeind, E., Bergmann, M., Budaeva, N., Hoste, E., Jaekisch, N., von Juterzenka, K., Matthiessen, J., Mokievsky, V., Nöthig, E.-M., Quéric, N.-V., Sablotny, B., Sauter, E., Schewe, I., Urban-Malinga, B., Wegner, J., Wlodarska-Kowalczuk, M., Klages, M., 2005. HAUSGARTEN multidisciplinary investigations at a deep-sea, long-term observatory in the Arctic Ocean. Oceanography (Wash. D. C.) 18, 46–61.

Soltwedel, T., Grzelak, K., Hasemann, C., 2020. Spatial and temporal variation in deep-sea meiofauna at the LTER observatory HAUSGARTEN in the fram strait (Arctic ocean). Diversity 12, 1–23. https://doi.org/10.3390/d12070279.

Soltwedel, T., Hasemann, C., Vedenin, A., Bergmann, M., Taylor, J., Krauß, F., 2019b. Bioturbation rates in the deep fram strait: results from in situ experiments at the arctic LTER observatory HAUSGARTEN. J. Exp. Mar. Biol. Ecol. 511, 1–9.

Soltwedel, T., Jaeckisch, N., Ritter, N., Hasemann, C., Bergmann, M., Klages, M., 2009. Bathymetric patterns of megafaunal assemblages from the arctic deep-sea observatory HAUSGARTEN. Deep-Sea Res. I 56, 1856–1872. https://doi.org/10.1016/j.dsr.2009.05.012.

Soltwedel, T., Vopel, K., 2001. Bacterial abundance and biomass in response to organism-generated habitat heterogeneity in deep-sea sediments. Mar. Ecol. Prog. Ser. 219, 291–298.

Søreide, J.E., Leu, E., Berge, J., Graeve, M., Falk-Petersen, S., 2010. Timing of blooms, algal food quality and Calanus glacialis reproduction and groth in a changing Arctic. Glob. Change Biol. 16, 3154–3163. https://doi.org/10.1111/j.1365-2486.2010.02175.x.

Soto, E.H., Paterson, G.L.J., Billett, D.S.M., Hawkins, L.E., Galéron, J., Sibuet, M., 2010. Temporal variability in polychaete assemblages of the abyssal NE Atlantic Ocean. Deep-Sea Res. II, 1396–1405.

Stammerjohn, S., Massom, R., Rind, D., Martinson, D., 2012. Regions of rapid sea ice change: an inter-hemispheric seasonal comparison. Geophys. Res. Lett. 39, 1–8. https://doi.org/10.1029/2012GL050874.

Steele, M., Ermold, W., 2015. Loitering of the retreating sea ice edge in the arctic seas. J. Geophys. Res., Oceans 120, 7699–7721. https://doi.org/10.1002/2015JC011182.

Taylor, J., Krumpen, T., Soltwedel, T., Gutt, J., Bergmann, M., 2017. Dynamic benthic megafaunal communities: assessing temporal variations in structure, composition and diversity at the arctic deep-sea observatory HAUSGARTEN between 2004 and 2015. Deep-Sea Res. Part A Oceanogr. Res. Pap. 122, 81–94. https://doi.org/10.1016/j.dsr.2017.02.008.

Taylor, J., Krumpen, T., Soltwedel, T., Gutt, J., Bergmann, M., 2016. Regional- and local-scale variations in benthic megafaunal composition at the arctic deep-sea observatory HAUSGARTEN. Deep-Sea Res. Part A Oceanogr. Res. Pap. 108, 58–72. https://doi.org/10.1016/j.dsr.2015.12.009.

Taylor, J., Staufenbiel, B., Soltwedel, T., Bergmann, M., 2018. Temporal trends in the biomass of three epibenthic invertebrates from the deep-sea observatory HAUSGARTEN (Fram strait, Arctic Ocean). Mar. Ecol. Prog. Ser. 602, 15–29. https://doi.org/10.3354/meps12654.

Thistle, D., 2003. The deep-sea floor: an overview. In: Tyler, P.A. (Ed.), Ecosystems of the World. Elsevier Science, pp. 5–37.

Turner, J.T., 2002. Zooplankton fecal pellets, marine snow and sinking phytoplankton blooms. Aquat. Microb. Ecol. 27, 57–102. https://doi.org/10.3354/ame027057.

Van Oevelen, D., Bergmann, M., Soetaert, K., Bauerfeind, E., Hasemann, C., Klages, M., Schewe, I., Soltwedel, T., Budaeva, N.E., 2011. Carbon flows in the benthic food web at the deep-sea observatory HAUSGARTEN (Fram strait). Deep-Sea Res. Part A Oceanogr. Res. Pap. 58, 1069–1083. https://doi.org/10.1016/j.dsr.2011.08.002.

Vedenin, A., Mokievsky, V., Soltwedel, T., Budaeva, N., 2019. The temporal variability of the macrofauna at the deep-sea observatory HAUSGARTEN (Fram strait, Arctic Ocean). Polar Biol. 42, 527–540. https://doi.org/10.1007/s00300-018-02442-8.

von Appen, W.-J., 2018. In: The Expedition PS114 of the Research Vessel POLARSTERN to the Fram Strait in 2018, Berichte Zur Polar- Und Meeresforschung = Reports on Polar and Marine Research. https://doi.org/10.2312/BzPM_0723_2018. Bremerhaven, Germany.

von Appen, W.J., Waite, A.M., Bergmann, M., Bienhold, C., Boebel, O., Bracher, A., Cisewski, B., Hagemann, J., Hoppema, M., Iversen, M.H., Konrad, C., Krumpen, T., Lochthofen, N., Metfies, K., Niehoff, B., Nöthig, E.M., Purser, A., Salter, I., Schaber, M., Scholz, D., Soltwedel, T., Torres-Valdes, S., Wekerle, C., Wenzhöfer, F., Wietz, M., Boetius, A., 2021. Sea-ice derived meltwater stratification slows the biological carbon pump: results from continuous observations. Nat. Commun. 12. https://doi.org/10.1038/s41467-021-26943-z.

Wheatcroft, R.A., Smith, C.R., Jumars, P.A., 1989. Dynamics of surficial trace assemblages in the deep sea. Deep Sea Res. 36, 71–91. https://doi.org/10.1016/0198-0149(89)90019-8.

Wickham, H., 2016. ggplot2: Elegant Graphics for Data Analysis.

Wickham, H., François, R., Henry, L., Müller, K., Vaughan, D., 2023. Dplyr: a Grammar of Data Manipulation.

Wickham, H., Pedersen, T.L., Seidel, D., 2025. Scales: Scale Functions for Visualization.

Wickham, H., Vaughan, D., Girlich, M., 2024. Tidyr: Tidy Messy Data.

Wieking, G., Kröncke, I., 2005. Is benthic trophic structure affected by food quality? The Dogger Bank example. Mar. Biol. 146, 387–400. https://doi.org/10.1007/s00227-004-1443-2.

Wilke, C.O., Wiernik, B.M., 2022. Ggtext: Improved Text Rendering Support for "Ggplot2.".

WoRMS Editorial Board, 2024. World register of marine species. https://www.marinespecies.orgatVLIZ, 11.28.24.

Xie, Y., Allaire, J., Horner, J., 2025. Markdown: Render Markdown with "Commonmark.".

Zhulay, I., Iken, K., Renaud, P.E., Bluhm, B.A., 2019. Epifaunal communities across marine landscapes of the deep Chukchi borderland (Pacific arctic). Deep-Sea Res. Part A Oceanogr. Res. Pap. 151. https://doi.org/10.1016/j.dsr.2019.06.011.